



HAL
open science

One-dimensional mechanism of gaseous deflagration-to-detonation transition

Paul Clavin

► **To cite this version:**

Paul Clavin. One-dimensional mechanism of gaseous deflagration-to-detonation transition. *Journal of Fluid Mechanics*, 2023, 974, 10.1017/jfm.2023.751 . hal-04478202

HAL Id: hal-04478202

<https://hal.science/hal-04478202>

Submitted on 26 Feb 2024

HAL is a multi-disciplinary open access archive for the deposit and dissemination of scientific research documents, whether they are published or not. The documents may come from teaching and research institutions in France or abroad, or from public or private research centers.

L'archive ouverte pluridisciplinaire **HAL**, est destinée au dépôt et à la diffusion de documents scientifiques de niveau recherche, publiés ou non, émanant des établissements d'enseignement et de recherche français ou étrangers, des laboratoires publics ou privés.

Banner appropriate to article type will appear here in typeset article

1 **One-dimensional mechanism of gaseous** 2 **deflagration-to-detonation transition.**

3 **Paul Clavin**[†],

4 Aix Marseille Université, CNRS, Centrale Marseille, IRPHE UMR7342,
5 49 Rue F. Joliot Curie, 13384 Marseille, France

6 (Received xx; revised xx; accepted xx)

7 A one-dimensional mechanism of deflagration to detonation transition (DDT) is identified
8 and investigated by an asymptotic analysis in the double limit of large activation energy
9 and small Mach number of the laminar flame velocity. The unsteady analysis concerns the
10 self-accelerating tip of an elongated flame in a smooth walled tube. The flame on the tip,
11 considered as plane and orthogonal to the tube axis, is pushed from behind by the longitudinal
12 back-flow resulting from the cumulative effect of the radial flows of burned gas issued from
13 the lateral flame of the finger-like front. The analysis of the one-dimensional dynamics
14 is performed by coupling the flame structure with the downstream-running compression
15 waves propagating in the external flows. A critical elongation is identified from which the
16 slightest increase in elongation leads to a pressure run-away producing the flame blow-off.
17 The dynamics of the inner structure of the laminar flame on the tip which is accelerated by
18 the self-induced back-flow is characterized by a finite-time singularity of the reacting flow
19 in the form of a dynamical saddle-node bifurcation.

20 **Key words:**

21 **1. Introduction**

22 Deflagration-to-detonation transition (DDT) is observed in tubes filled with energetic gaseous
23 mixtures such as stoichiometric hydrogen-oxygen or acetylene-oxygen mixtures. DDT is a
24 fascinating phenomenon of abrupt transition (in less than a microsecond) between two
25 opposite regimes of propagation, a markedly subsonic flame and a supersonic combustion
26 wave. A detonation is a supersonic wave consisting in a smooth front of a strong inert
27 shock followed by a thin reaction zone (including induction) across which viscosity, heat
28 conduction and molecular diffusion of species are negligible. The overpressure is large, the
29 pressure ratio ranging from 15 to 50. By comparison, each surface element of the brush of a
30 turbulent flame is a quasi-isobaric reaction-diffusion wave whose velocity relative to the gas
31 (laminar flame velocity) is much smaller than the sound speed, typically by a factor 10^{-2} .
32 However, due to the increase in surface area of the wrinkled front, the speed of the flame

[†] Email address for correspondence: paul.clavin@univ-amu.fr

33 brush (measured in the laboratory frame) becomes large, not far from the sound speed near
34 the transition.

35 The pioneering experiments of Urtiew & Oppenheim (1966) have shown that the DDT
36 onset is a local phenomenon occurring in a "small explosion center" either on a surface
37 element of the flame brush or in the viscous boundary layer ahead of the flame. We will not
38 consider the latter case for which the DDT is more likely due to the gradient mechanism
39 of Zeldovich (1980) reinforced by compressional heating, as discussed p. 260 in Clavin &
40 Searby (2016) and observed in sub-millimeter tubes by the numerical simulation of Houim
41 *et al.* (2016). In the following, the attention is focused on the first case for which the
42 explosion center is on the flame outside the boundary layer. The origin and nature of the
43 explosion centers remained unexplained. After more than a century of experimental works
44 and decades of numerical studies, DDT is not yet understood, see textbooks, Lee (2008)
45 and Clavin & Searby (2016) for example. Despite various attempts, there is no fundamental
46 mechanism that is generally agreed upon as being universal. Neither the role of turbulence
47 mentioned by Shchelkin & Troshin (1965) nor the gradient of induction time of Zeldovich
48 (1980) are involved in the experiments and numerical simulations of Liberman *et al.* (2010),
49 Kuznetsov *et al.* (2010) and Ivanov *et al.* (2011). These seminal works concern DDT of
50 flames propagating in smooth walled tubes in which the induced flow of unburned gas is
51 laminar in the bulk, the 3 mm boundary layer staying stuck at the wall near the flame, see
52 p. 692 in Liberman *et al.* (2010). The detonation onset in these experiments is a local and
53 sudden phenomenon occurring in a "small explosion center" on the flame front outside the
54 boundary layer without any reflected shock (long tubes). Therefore the transition appears to
55 be an intrinsic mechanism of a laminar flame accelerated by a self-induced flow. The DDT
56 was also observed by Wu *et al.* (2007) and Wu & Wang (2011) in micro-scale tubes (0.5 mm
57 radius) in which the transition concerns very elongated fronts of laminar flame. Kuznetsov
58 *et al.* (2010), Ivanov *et al.* (2011) and Bykov *et al.* (2022) mentioned that the shocks formed
59 in the immediate proximity ahead of the self-accelerating flame are suddenly overtaken by
60 the reaction front. A striking observation is that the Mach number of these shocks is not larger
61 than 2.5 so that the temperature of the compressed gas is not large enough for self-igniting
62 the reactive mixture, ruling out the both DDT mechanisms of Shchelkin & Troshin (1965)
63 and Zeldovich (1980).

64 A key mechanism underlying the DDT was identified long ago by Deshaies & Joulin
65 (1989). Treating a turbulent flame brush as a planar discontinuity propagating at a subsonic
66 velocity equal to the laminar flame velocity multiplied by a wrinkling factor σ , Deshaies
67 & Joulin (1989) investigated the self-similar solutions characterized by a constant velocity
68 of the weak shock ahead of the flame. They showed that, due to a laminar flame velocity
69 highly sensitive to temperature changes, the self-similar solutions no longer exist above a
70 critical value of σ close to ten. The assumption of a weak shock used by Deshaies & Joulin
71 (1989) can be easily removed without modifying qualitatively the result. The turning point
72 of the curve "self-similar solution versus σ " is due to a nonlinear thermal feed-back loop: the
73 laminar flame velocity is a function of the temperature which increases with the strength of
74 the lead shock, the latter increasing in turn with the flame velocity. This pioneering analysis
75 was overlooked by the combustion community during more than twenty years. A weaknesses
76 of the self-similar solutions is the steady and uniform state of unburned gas flow between
77 the flame and the lead shock. A basic ingredient of the DDT is overlooked, namely the
78 unsteady flow of the compression waves generated by the accelerating flame. The role of the
79 flame acceleration has been invoked in the past but with no connection to the turning point of
80 Deshaies & Joulin (1989). However, in a series of articles starting nearly 10 years ago, Kagan
81 & Sivashinsky (2017), motivated by the work of Deshaies & Joulin (1989), have investigated
82 numerically the one-dimensional propagation of a laminar flame ignited at the closed-end of

83 a tube and sustained by a reaction rate which is increased artificially by a factor σ^2 . For values
 84 of σ above a critical value about 10, namely close to the critical condition of Deshaies &
 85 Joulin (1989), the numerical results of Kagan & Sivashinsky (2017) show a sharp transition
 86 to detonation few time after a quasi-isobaric ignition. An exothermic reaction rate which is
 87 a hundred times larger than the inelastic collision frequency of molecules associated with a
 88 large activation energy cannot describe real flames. Nevertheless, the numerical findings of
 89 Kagan & Sivashinsky (2017) are useful for improving our understanding of DDT: they suggest
 90 a runaway of the one-dimensional structure of "fast" laminar flames, still markedly subsonic,
 91 resulting from the strong interaction near the turning point of Deshaies & Joulin (1989)
 92 between the acceleration-induced compression waves and the reaction-diffusion mechanisms
 93 sustaining a quasi-isobaric combustion wave.

94 The objective of the present paper is an attempt to describe theoretically such a one-
 95 dimensional DDT mechanism on the tip of a self-accelerating elongated flame using a
 96 combustion rate compatible with the kinetic theory of gas for a one-step Arrhenius law
 97 with a large activation energy. In order to enlighten the essential features, the problem
 98 will be over-simplified, keeping only the key mechanisms responsible for the spontaneous
 99 transition. The one-dimensional model is inspired by the schematic analysis of Clanet &
 100 Searby (1996) who treat the tip of the elongated front as a planar flame orthogonal to the
 101 tube axis while the side of the finger-like flame is quasi-parallel to the adiabatic tube wall.
 102 An essential ingredient for the DDT on the tip is the longitudinal back-flow of burned gas
 103 generated by the cumulative effects of the combustion of the lateral side of the elongated
 104 flame front, see figure 1. This flow hits the flame on the tip from the burned-gas side with
 105 a flow velocity u_b proportional to both the flame elongation and the laminar flame velocity
 106 U_b . If the flame on the tip is treated as a discontinuity, the self-similar solutions present a
 107 turning point similar to that of Deshaies & Joulin (1989) for a turbulent wrinkled flame,
 108 the elongation of the finger front playing the role of the wrinkling factor σ . According to
 109 Clavin & Tofaili (2021), the critical condition is in good agreement with the DDT observed
 110 in the experiments of Liberman *et al.* (2010) and Kuznetsov *et al.* (2010). The back-flow
 111 u_b increasing with the elongation of the finger-like flame, the speed of the tip relatively to
 112 the tube $U_P = u_b + U_b$ increases also. Therefore, the flame acting as a semi-transparent
 113 piston, compression waves are generated in the unburned gas. Still considering the flame as
 114 a discontinuity, the analysis has been recently extended beyond self-similarity to take into
 115 account the acceleration-induced transient flow in the unburned gas, see Clavin (2022) and
 116 Clavin & Champion (2022). A singularity of the flow gradient appears suddenly on the flame
 117 front when the elongation reaches the critical value while the velocity of the flame front, the
 118 pressure and the flame temperature remain finite. Even though no runaway of temperature
 119 and/or pressure is described by these preliminary analyses, the finite-time singularity of the
 120 flow gradient on the flame front suggests the existence of a fundamental DDT mechanism. In
 121 the present article, the analysis is further extended to the inner structure of the laminar flame
 122 by coupling the unsteady reaction-diffusion mechanisms controlling the flame structure to
 123 the downstream-running compression waves in the external flows. The solution demonstrates
 124 that a one-dimensional DDT mechanism exists in the form of a finite-time singularity of the
 125 reacting flow leading to blow off the inner structure of the laminar flame on the tip. More
 126 precisely, the singularity takes the form of a dynamical saddle node bifurcation presented
 127 in classical textbooks of applied mathematics such as Binder & Orszag (1984) or Strogatz
 128 (1994). The key physical mechanism turns out to be the divergence of the flame acceleration
 129 that occurs systematically at the turning point for a small elongation rate as tiny as it may be.
 130 The turning point being associated with the nonlinear thermal feedback mentioned earlier,
 131 the critical condition has nothing to do with the CJ deflagration (sonic condition in the burned
 132 gas flow) mentioned in the DDT literature for turbulent flames in tubes filled with obstacles.

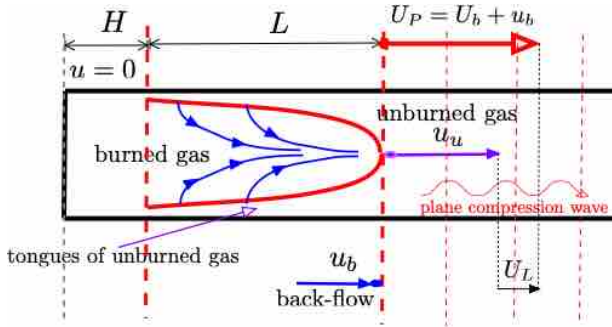


Figure 1: Sketch of the burned gas flow in an elongated flame. The curved flame front propagating without deformation in a tube is characterized by $dL/dt \approx 0$ and $dH/dt \approx U_p$. The planar lead shock associated with the constant unburned gas flow u_u is far away from the flame tip. Downstream running compression waves are launched in the unburned gas by the accelerating front as soon as the elongation increases so that the gas temperature is increased on the flame by adiabatic compression. Due to the nonlinear thermal feedback mentioned in the text, a drastic effect is produced at the critical flame velocity $U_P = U_P^*$ because the flame acceleration $dU_P/dt|_{U_P=U_P^*}$ diverges even when the elongation rate is small $dL/dt \ll U_P^*$. It is shown in this article that a finite time singularity of the reacting flow occurs on the tip for $U_P(t)$ slightly larger than U_P^* .

133 Such a sonic condition can never exist on the burned gas side of laminar flames constituting
 134 the turbulent flame brush.

135 Unfortunately from a theoretical point of view, there is no satisfactory theory for the
 136 unsteady curved flow of burned gas sketched in figure 1. Hopefully a detailed analysis of the
 137 burnt gas flow is not needed for understanding the finite-time singularity. In the following,
 138 a small elongation rate is prescribed and a crude model for the unsteady back-flow is used.
 139 In this context, an asymptotic analysis of the dynamics of the quasi-planar flame on the tip
 140 is then performed in the distinguished limit of large activation energy, small Mach number
 141 of the laminar flame and small elongation rate (smaller than the inverse of the transit time
 142 of fluid particles across the inner structure of the flame), the elongation having the same
 143 order of magnitude as the wrinkling factor in Deshaies & Joulin (1989). A similar analytical
 144 study can also be performed with a multiple-step chemical network representative of gaseous
 145 combustion if the production of the main radical is located in a thin reaction zone inside
 146 the inner flame structure, as it is usually the case. The essential point is the strong thermal
 147 sensitivity of the laminar flame velocity $(T/U_b)dU_b/dT \gg 1$. Considering an elongated
 148 flame as a constitutive element of cellular flames, the DDT scenario could be relevant for
 149 wrinkled flames in tubes as well as for unstable flames expanding freely in open space.

150 The basic equations are recalled in § 2. The formulation of the problem is presented in
 151 § 3 where the back-flow models are introduced. The asymptotic method is presented in § 4.
 152 Matching the quasi-isobaric flow in the flame structure (small length-scale) with the external
 153 compressible flows is performed in § 5 where a general relation is obtained linking the flow
 154 in an unsteady flame structure, the pressure and the flame temperature. The normal form of a
 155 dynamical saddle-node bifurcation describing the finite-time runaway of pressure and flame
 156 temperature is first derived in § 6 for a flame structure in steady state. A similar result is
 157 obtained in the more technical analysis of § 7 taking into account the unsteady inner structure
 158 of the laminar flame. Discussion and conclusion are presented in § 8.

159 **2. The basic equations**

160 A one-dimensional time-dependent combustion flow of an ideal gas is considered in a planar
 161 geometry with x denoting the coordinate in the flow direction and t the time. The propagation
 162 is from left to right.

163 *2.1. Conservative form*

164 The equations for mass and momentum are

$$165 \quad \frac{\partial \rho}{\partial t} = -\frac{\partial(\rho u)}{\partial x}, \quad \frac{\partial(\rho u)}{\partial t} = -\frac{\partial[p + \rho u^2 - \mu \partial u / \partial x]}{\partial x} \quad (2.1)$$

166 where ρ , p and u are respectively the density, the pressure and the velocity of the flow
 167 in the laboratory frame and μ is the viscosity. For the sake of simplicity we will consider
 168 an irreversible one-step exothermal reaction. This simplification can be removed and the
 169 fundamental result does not depend qualitatively on a detailed chemical scheme provided
 170 the laminar flame velocity is highly sensitive to the temperature. Introducing the progress
 171 variable Y , namely the mass fraction of products, $Y = 0$ in the unburned mixture and $Y = 1$
 172 in the burned gas), the chemical heat release per unit mass q_m , the heat conductivity λ and
 173 the diffusion coefficient D , the equation for energy, written in conservative form, is

$$174 \quad \frac{\partial[\rho(c_v T + u^2/2 - q_m Y)]}{\partial t} = \quad (2.2)$$

$$175 \quad -\frac{\partial[\rho u(c_v T + p/\rho + u^2/2 - q_m Y) - \lambda \partial T / \partial x - \mu u \partial u / \partial x + q_m \rho D \partial Y / \partial x]}{\partial x}$$

176 with the perfect gas law, $p = c_v(\gamma - 1)\rho T = nk_B T$ in which k_B is the Boltzmann constant
 177 and n the molecular density. The ratio of specific heats $\gamma \equiv c_p/c_v$ is assumed constant for
 178 simplicity. The conservation equation of species for a one-step reaction, written in terms of
 179 the progress variable, $Y \in [0, 1]$ reads

$$180 \quad \frac{\partial(\rho Y)}{\partial t} = -\frac{\partial[\rho u Y - \rho D \partial Y / \partial x]}{\partial x} + \rho W(Y, T) \quad (2.3)$$

181 with a reaction rate in the form of an Arrhenius law for a large activation energy $\mathcal{E} \gg k_B T$,
 182 proportional to the frequency of binary collisions $1/t_{coll}$

$$183 \quad W(Y, T) = \frac{B}{t_{coll}} (1 - Y)^2 e^{-\mathcal{E}/k_B T}. \quad (2.4)$$

184 These macroscopic equations are solutions of the Boltzmann equation in the hydrodynamic
 185 limit (macroscopic length scales larger than the mean free path and time larger than t_{coll}
 186 respectively). The solution shows how the frequency of binary collisions $1/t_{coll}$, the diffusion
 187 coefficient D and the sound speed $a = \sqrt{\gamma p/\rho}$ are related in a perfect gas $p = nk_B T$

$$188 \quad D = \frac{1}{6\sqrt{\gamma} n r_o^2} a, \quad \frac{D}{t_{coll}} = \frac{8\sqrt{\pi}}{3\gamma} a^2, \quad (2.5)$$

189 r_o being the radius of the molecules. The parameter B , usually called the pre-factor, is the
 190 reduced activation energy times the initial molecular dilution of reactant y_i

$$191 \quad B = y_i \frac{\mathcal{E}}{k_B T} \quad \Rightarrow \quad B \frac{D}{t_{coll}} = \frac{8\sqrt{\pi}}{3} y_i \frac{\mathcal{E}}{m}. \quad (2.6)$$

Equations (2.5)-(2.6) are useful to express the laminar flame velocity in terms of the flame temperature. For the sake of simplicity the molecules of reactants, products and diluent are assumed to have the same mass m ($\rho = nm$) and the same radius r_0 .

According to the asymptotic analysis of Zeldovich-Frank-Kamenetskii (ZFK) in the limit of large activation energy $\mathcal{E}/k_B T_b \gg 1$, the laminar flame velocity $U_b(T_b)$ relative to the burned gas denoted by the subscript b (T_b is the flame temperature) takes the form

$$U_b(T_b) = \frac{1}{\tilde{\beta}_b^{3/2}} \sqrt{8B_b \frac{D_b}{t_{coll b}} e^{-\mathcal{E}/k_B T_b}}, \quad \text{where} \quad \tilde{\beta}_b \equiv \frac{q_m}{c_p T_b} \frac{\mathcal{E}}{k_B T_b}, \quad (2.7)$$

showing how small is the Mach number of the laminar flame velocity

$$\varepsilon \equiv \frac{U_b}{a_b} = \sqrt{\frac{2! 16 \pi^{1/2}}{3\gamma}} y_i \frac{1}{\tilde{\beta}_b^{3/2}} \sqrt{\frac{\mathcal{E}}{k_B T_b}} e^{-\mathcal{E}/2k_B T_b}, \quad (2.8)$$

see a didactic presentation in Clavin & Searby (2016). Typical orders of magnitude in real flames are $U_b/a_b \approx 10^{-3} - 10^{-2}$. Equation (2.8) leads to similar values $\varepsilon \approx 10^{-3}$ for $\mathcal{E}/k_B T_b \approx 10$, $q_m/c_p T_b \approx 0.8$ and $\varepsilon \approx 10^{-2}$ for smaller values of $\mathcal{E}/k_B T_b$ as it is the case in energetic mixtures. According to (2.5)-(2.8), the ratio of the laminar flame velocity for two flames with different temperatures takes the form

$$\frac{U_b(T_{b1})}{U_b(T_{b2})} = \left(\frac{T_{b1}}{T_{b2}}\right)^3 \exp\left[-\frac{\mathcal{E}}{2k_B} \left(\frac{1}{T_{b1}} - \frac{1}{T_{b2}}\right)\right]. \quad (2.9)$$

The main effect of a complex network of chemical kinetics is to modify the power law in the Arrhenius pre-factor and to introduce a temperature cutoff $T_c \in [850 - 1200K]$ below which the combustion cannot proceed. In addition, the activation energy \mathcal{E} varies with the temperature for $T > T_c$. For a large activation energy $\mathcal{E}/(k_B T_b) \gg 1$ and far from the chemical quenching $T_b > T_c$, the temperature variation of \mathcal{E} can be neglected in a limited range of flame temperature $\Delta T_b \ll \mathcal{E}/(d\mathcal{E}/dT_b)$. The upper bound of $\Delta T_b/T_b$ for the validity of this inequality is not small when the relative variation of the activation energy is smaller than the reduced activation energy $(T_b/\mathcal{E})d\mathcal{E}/dT_b < \mathcal{E}/k_B T_b$. In such conditions, equation (2.9) is reduced to an Arrhenius law

$$\beta \gg 1, \quad \frac{\mathcal{E}}{k_B T_{b2}} \left(\frac{T_{b1}}{T_{b2}} - 1\right) = O(1) : \quad \frac{U_b(T_{b1})}{U_b(T_{b2})} \approx \exp\left[\frac{\mathcal{E}/2}{k_B T_{b2}} \left(\frac{T_{b1}}{T_{b2}} - 1\right)\right]. \quad (2.10)$$

However in highly reactive mixtures (stoichiometric H_2 or C_2H_4 mixtures in pure oxygen) the flame temperature is large and the reduced activation energy is of order unity so that the power law $(T_{b1}/T_{b2})^3$ in (2.9) cannot be ignored.

2.2. Non-dimensional equations in the Lagrangian form

From now on, the reference state used in the non-dimensional equations is the burned gas of the steady flame at the initial condition (labelled i). The latter is a self-similar solution with the lead shock at infinity. Denoting T_{ui} and ρ_{bi} respectively the temperature of the unburned gas and the density of the burned gas in the initial state, the reference temperature, velocity, density and pressure are

$$T_{ref} = T_{bi} = T_{ui} + q_m/c_p, \quad U_{ref} = U_b(T_{bi}), \quad \rho_{ref} = \rho_{bi}, \quad p_{ref} = (c_p - c_v)\rho_{ref}T_{ref}. \quad (2.11)$$

Using the corresponding flame thickness and transit time $d_{ref} = D_{ref}/U_{ref}$ and $t_{ref} = d_{ref}/U_{ref} = D_{ref}/U_{ref}^2$ where D_{ref} is the molecular diffusion coefficient in the reference state,

229 the following non-dimensional variables are introduced

$$230 \quad \tau \equiv t/t_{\text{ref}}, \quad \xi \equiv (x - X_P)/d_{\text{ref}}, \quad \text{where} \quad t_{\text{ref}} \equiv d_{\text{ref}}/U_{\text{ref}} = D_{\text{ref}}/U_{\text{ref}}^2, \quad (2.12)$$

$$231 \quad r \equiv \frac{\rho}{\rho_{\text{ref}}}, \quad v \equiv \frac{u}{U_{\text{ref}}}, \quad \pi \equiv \frac{p}{p_{\text{ref}}}, \quad \theta \equiv \frac{T}{T_{\text{ref}}}, \quad v_P \equiv \frac{U_P}{U_{\text{ref}}}, \quad (2.13)$$

232 where $x = X_P(t)$ is the instantaneous position of the flame (for example, the maximum
233 of reaction rate), $u(x, t)$ and $U_P(t) \equiv dX_P/dt$ are respectively the flow velocity and the
234 propagation speed of the flame in the laboratory frame (not to be confused with the laminar
235 flame velocity U_b). The non-dimensional mass flux across the flame $m \equiv \rho(U_P - u)/\rho_{\text{ref}}U_{\text{ref}}$
236 takes the form

$$237 \quad m(\xi, \tau) = r[v_P(\tau) - v(\xi, \tau)] > 0, \quad r \equiv \pi/\theta. \quad (2.14)$$

238 Introducing the Mach number of the laminar flame, the reduced heat release and the reduced
239 activation energy

$$240 \quad \varepsilon \equiv \frac{U_{\text{ref}}}{a_{\text{ref}}} \approx 10^{-2}, \quad q \equiv \frac{q_m}{c_p T_{\text{ref}}} \approx 0.7, \quad \beta \equiv \frac{\mathcal{E}}{k_B T_{\text{ref}}} = 4 - 8, \quad (2.15)$$

241 and using the relations $1/(\rho_{\text{ref}}c_p T_{\text{ref}}) = (\gamma - 1)/(\gamma p_{\text{ref}}) = (\gamma - 1)/(\rho_{\text{ref}}a_{\text{ref}}^2)$ and $D_{\text{ref}} =$
242 $\lambda/(\rho_{\text{ref}}c_p) = \mu/\rho_{\text{ref}}$ ($Le=1$ for simplicity), the non-dimensional Lagrangian form of (2.1)-
243 (2.4), written in the frame moving with the flame $t_{\text{ref}}\partial/\partial t \rightarrow \partial/\partial\tau - v_P\partial/\partial\xi$, reads

$$244 \quad \frac{\partial r}{\partial\tau} = \frac{\partial m}{\partial\xi}, \quad r = \pi/\theta \quad (2.16)$$

$$245 \quad \frac{\partial v}{\partial\tau} - m\frac{\partial v}{\partial\xi} = -\frac{1}{\gamma\varepsilon^2}\frac{\partial\pi}{\partial\xi} + \frac{\partial^2 v}{\partial\xi^2} \quad (2.17)$$

$$246 \quad \left[r\frac{\partial}{\partial\tau} - m\frac{\partial}{\partial\xi} \right] Y - \frac{\partial^2 Y}{\partial\xi^2} = w(\theta, Y) \quad (2.18)$$

$$247 \quad \left[r\frac{\partial}{\partial\tau} - m\frac{\partial}{\partial\xi} \right] \theta - \frac{(\gamma - 1)}{\gamma} \left[\frac{\partial}{\partial\tau} + [v - v_P]\frac{\partial}{\partial\xi} \right] \pi =$$

$$248 \quad \frac{\partial^2 \theta}{\partial\xi^2} + (\gamma - 1)\varepsilon^2 \left(\frac{\partial v}{\partial\xi} \right)^2 + q w. \quad (2.19)$$

249 For a large activation energy, the non-dimensional reaction rate takes the form,

$$250 \quad w(\theta, Y) \equiv t_{\text{ref}}w = \frac{\beta_{\text{ref}}^3 \pi_b}{8 \theta_b} (1 - Y)^2 \exp \left[\frac{\mathcal{E}}{k_B T_{\text{ref}}} (\theta - 1) \right], \quad \beta_{\text{ref}} \equiv \frac{q_m}{c_p T_{\text{ref}}} \frac{\mathcal{E}}{k_B T_{\text{ref}}} \quad (2.20)$$

251 the subscript b denoting the burned gas. Eliminating the density by using the perfect gas
252 law $r = \pi/\theta$, the four equations (2.16)-(2.19) concern four fields $v(\xi, \tau)$, $\pi(\xi, \tau)$, $Y(\xi, \tau)$ and
253 $\theta(\xi, \tau)$ plus an unknown function $v_P(\tau)$ appearing in the mass flux $m(\xi, \tau)$ (2.14).

254 2.3. Mass-weighted coordinate

255 The analysis of the unsteady flame structure is more easily performed using the mass-
256 weighted coordinate z and the reduced mass flux at the origin ($z = 0$) $m(\tau) \equiv m(z = 0, \tau)$
257 with, according to (2.14),

$$258 \quad m(\tau) = r(0, \tau)[v_P(\tau) - v(0, \tau)] = \frac{\pi(0, \tau)}{\theta(0, \tau)} [v_P(\tau) - v(0, \tau)] > 0. \quad (2.21)$$

259 Introducing the change of variables $(\xi, \tau) \rightarrow (z, \tau)$

$$260 \quad z \equiv \int_0^\xi r(\xi', \tau) d\xi', \quad \frac{\partial}{\partial \xi} = r \frac{\partial}{\partial z} = \frac{\pi}{\theta} \frac{\partial}{\partial z}, \quad (2.22)$$

$$261 \quad \left. \frac{\partial}{\partial \tau} \right|_\xi = \left. \frac{\partial}{\partial \tau} \right|_z + \left[\int_0^\xi \frac{\partial r(\xi', \tau)}{\partial \tau} d\xi' \right] \frac{\partial}{\partial z} = \left. \frac{\partial}{\partial \tau} \right|_z + [m(\xi, \tau) - m(\tau)] \frac{\partial}{\partial z} \quad (2.23)$$

$$262 \quad (v - v_P(\tau)) \frac{\partial}{\partial \xi} = -m(\xi, \tau) \frac{\partial}{\partial z} \Rightarrow \left. \frac{\partial}{\partial \tau} \right|_\xi + (v - v_P(\tau)) \frac{\partial}{\partial \xi} = \left. \frac{\partial}{\partial \tau} \right|_z - m(\tau) \frac{\partial}{\partial z} \quad (2.24)$$

263 where the function $m(\tau)$ in front of the derivative with respect to z depends only on the time.
264 Continuity (2.16) written with the variables (z, τ)

$$265 \quad r \frac{\partial m(z, \tau)}{\partial z} = \frac{\partial r(z, \tau)}{\partial \tau} + [m(z, \tau) - m(\tau)] \frac{\partial r}{\partial z} \quad (2.25)$$

266 yields after multiplication by $1/r^2$

$$267 \quad \frac{1}{r} \frac{\partial m(z, \tau)}{\partial z} = - \left. \frac{\partial(1/r)}{\partial \tau} \right|_z - [m(z, \tau) - m(\tau)] \frac{\partial(1/r)}{\partial z} \quad (2.26)$$

268 to give, using (2.14) $m(z, \tau) = -r(z, \tau)[v(z, \tau) - v_P(\tau)] > 0$,

$$269 \quad \frac{\partial m(z, \tau)}{\partial z} = -[v(z, \tau) - v_P(\tau)] \frac{\partial r}{\partial z} - r \frac{\partial v}{\partial z} \Rightarrow \frac{\partial v}{\partial z} = \left. \frac{\partial(1/r)}{\partial \tau} \right|_z - m(\tau) \frac{\partial(1/r)}{\partial z} \quad (2.27)$$

270 yielding the gradient of the flow in terms of $1/r = \theta(z, \tau)/\pi(z, \tau)$. For simplicity, the
271 diffusion coefficient D have been assumed to verify $\rho^2 D = \text{constant}$, $\partial(\rho D \partial/\partial x)/\partial x \rightarrow$
272 $(\rho^2 D/\rho_{\text{ref}}^2 D_{\text{ref}}) r \partial^2/\partial z^2 = r \partial^2/\partial z^2$. Then, (2.16)-(2.19) yield

$$273 \quad \frac{\partial v}{\partial z} = \left[\frac{\partial}{\partial \tau} - m(\tau) \frac{\partial}{\partial z} \right] \frac{\theta}{\pi},$$

$$274 \quad = \frac{1}{\pi} \left[\frac{\partial}{\partial \tau} - m(\tau) \frac{\partial}{\partial z} \right] \theta - \frac{\theta}{\pi^2} \left[\frac{\partial}{\partial \tau} - m(\tau) \frac{\partial}{\partial z} \right] \pi \quad (2.28)$$

$$275 \quad \left[\frac{\partial v}{\partial \tau} - m(\tau) \frac{\partial v}{\partial z} - \frac{\partial^2 v}{\partial z^2} \right] = - \frac{1}{\gamma \varepsilon^2} \frac{\partial \pi}{\partial z} \quad (2.29)$$

$$276 \quad \left[\frac{\partial Y}{\partial \tau} - m(\tau) \frac{\partial Y}{\partial z} - \frac{\partial^2 Y}{\partial z^2} \right] = w(\theta, Y), \quad Y(z, \tau) \in [0, 1] \quad (2.30)$$

$$277 \quad \left[\frac{\partial \theta}{\partial \tau} - m(\tau) \frac{\partial \theta}{\partial z} - \frac{\partial^2 \theta}{\partial z^2} \right] = qw(\theta, Y) + \frac{(\gamma - 1)\theta}{\gamma} \frac{1}{\pi} \left[\frac{\partial \pi}{\partial \tau} - m(\tau) \frac{\partial \pi}{\partial z} \right]$$

$$278 \quad + (\gamma - 1)\varepsilon^2 \left(\frac{\partial v}{\partial z} \right)^2 \quad (2.31)$$

279 where the perfect gas law $r = \pi/\theta$ has been used to eliminate the density. When the dissipative
280 terms (heat conduction, viscosity and reaction rate) are neglected, equation for energy (2.31)
281 takes the form of the entropy wave in an inert gas

$$282 \quad \frac{1}{\theta} \left[\frac{\partial \theta}{\partial \tau} - m(\tau) \frac{\partial \theta}{\partial z} \right] - \frac{(\gamma - 1)}{\gamma} \frac{1}{\pi} \left[\frac{\partial \pi}{\partial \tau} - m(\tau) \frac{\partial \pi}{\partial z} \right] = 0. \quad (2.32)$$

283 3. Formulation of the problem

284 Ignited at the closed end of a smooth walled tube, a laminar flame takes an elongated shape
 285 with a curved flow of burned gas striking the flame on the tip from behind (back-flow)
 286 sketched in figure 1. The attention is focused few time after the formation of the tulip flame
 287 when the finger shaped flame front is recovered and evolves slowly. Two basic mechanisms
 288 are involved in the DDT on the tip of the elongated flame: firstly the increase of the back-
 289 flow of burned gas on the tip $u_b(t)$ with both the elongation and the laminar flame velocity,
 290 and secondly the increase of the laminar flame velocity with the flame temperature. In the
 291 following, the elongation of the finger flame $S(\tau)$ is a given increasing function of the time
 292 $dS(\tau)/d\tau > 0$ starting at $\tau = 0$ from a self-similar solution whose elongation is $S_i \equiv S(0) \geq 1$.
 293 The increase rate is assumed smaller than the inverse of the transit time of a fluid particle
 294 across the flame,

$$295 \quad S(\tau) = [1 + \epsilon\tau]S_i, \quad \text{with} \quad \epsilon \ll \epsilon \ll 1. \quad (3.1)$$

296 The relation $\epsilon \ll \epsilon$ is useful to take into account unsteady effects while neglecting the terms
 297 of order ϵ^2 . As we shall see, a finite-time singularity of the flow is predicted for any $\epsilon > 0$,
 298 as small it can be. Under the condition (3.1), the curvature of the flame is negligible and the
 299 compression waves are quasi-planar if the tube radius r is in the range $\epsilon(r/d) = O(1)$.

300 3.1. Back-flow models

301 The flame on the tip is treated as planar and orthogonal to the propagation axis. Following
 302 Clanet & Searby (1996), the longitudinal gradient of burned gas flow on the tube axis $u(x, t)$
 303 is roughly modeled by a source term of mass whose origin is the burning of the lateral flame
 304 parallel to the wall. Denoting the laminar flame velocity (relative to the burned gas) of this
 305 lateral flame $U_{bw}(x, t)$, the gradient of the flow on the tube axis $u(x, t)$ is approximated by a
 306 one-dimensional mass conservation in an incompressible flow

$$307 \quad \frac{\partial u}{\partial x} = \frac{2}{R} U_{bw}(x, t) \quad (3.2)$$

308 where R is the radius of the tube. The longitudinal back-flow $u_b(t)$ impinging the tip from
 309 behind is obtained by integration along the axis of the finger flame. For a closed-end tube on
 310 the burned gas side, assuming that the incompressible flow of burned gas is at rest behind
 311 the elongated flame, one gets

$$312 \quad u_b(t) \equiv u(x = X_p(t), t) = \frac{2}{R} \int_{X_p-L}^{X_p} U_{bw}(x, t) dx \quad (3.3)$$

313 where $X_p(t)$ is the position of the tip and $L(t)$ the length of the elongated flame. Neglecting
 314 both the heat loss on the wall and the unsteadiness of the burned gas flow treated as
 315 incompressible, U_{bw} is uniform along the lateral flame and equal to the laminar flame
 316 speed on the tip at the same time $U_{bw} = U_b(t)$. Moreover, if the unsteadiness of the inner
 317 flame structure is negligible, $U_b(t)$ is given by (2.7)-(2.10) $U_b(t) = U_b(T_b(t))$. Under these
 318 approximations, the back-flow takes the form introduced by Clavin & Tofaili (2021),

$$319 \quad \text{instantaneous back-flow model: } u_b(t) = S(t) U_b(t), \quad U_b(t) \equiv U_b(T_b(t)), \quad (3.4)$$

320 where S is the elongation of the finger flame ($S = 2L/R$ in cylindrical geometry) and
 321 $T_b(t) = T_u(t) + Q/c_p$ where $T_u(t)$ is the temperature of the fresh mixture just ahead of the
 322 flame.

323 Unsteadiness of the flow of burned gas in an elongated flame is too complicated to
 324 be described analytically. Hopefully a detailed study is not useful in the following. This

325 unsteady effect will be roughly modeled by a delay $\Delta t(X_P - x)$ for transferring to the tip the
 326 flow of burned gas issued from the lateral flame at a distance $X_P - x$ from the tip,

$$327 \quad u_b(t) \approx \frac{2}{R} \int_{X_P-L}^{X_P} U_b(t - \Delta t(X_P - x)) dx. \quad (3.5)$$

328 Assuming a slow evolution of the laminar flame velocity $U_b/(dU_b/dt) \gg \Delta t(L) \geq \Delta t(X_P -$
 329 $x)$, a Taylor expansion yields

$$330 \quad u_b(t) \approx \frac{2L(t)}{R} U_b(t) - \frac{2}{R} \frac{dU_b}{dt} \int_{X_P-L}^{X_P} \Delta t(X_P - x) dx. \quad (3.6)$$

Assuming that the variation of the radial burned gas out of the lateral flames is propagated by
 the downstream-running compression waves with a quasi-constant sound speed a , $\Delta t(X_P -$
 $x) \approx (X_P - x)/a$,

$$\int_{X_P-L}^{X_P} \Delta t(X_P - x) dx \approx L^2/2a,$$

331 equation (3.6) yields, after introducing the overall delay $\Delta t_w \approx (1/2)L/a$,

$$332 \quad \text{delayed model of back-flow: } u_b(t) \approx S(t) \left[U_b(t) - \Delta t_w \frac{dU_b}{dt} \right] \approx S(t) U_b(t - \Delta t_w), \quad (3.7)$$

333 in which the variation with the time of Δt_w is a negligible second order effect.

334 3.2. Limit of large activation energy

335 The ZFK analysis in the limit of large activation energy, has been extended more than
 336 forty years ago to unsteady structure of flames, see Clavin & Searby (2016) for a didactic
 337 presentation. Choosing the instantaneous position of the reaction sheet as the origin on the
 338 z -axis and introducing the notation

$$339 \quad \beta \equiv \mathcal{E}/k_B T_{\text{ref}}, \quad \theta_b(\tau) \equiv T_b(t)/T_{\text{ref}} \quad (3.8)$$

340 for the reduced activation energy and the reduced flame temperature, the jump conditions on
 341 the reaction sheet take the form,

$$342 \quad z \leq 0 : \quad Y = 1, \\ 343 \quad z = 0 : \quad Y = 1, \quad \theta = \theta_b(\tau), \quad (\theta_b - 1) = O(1/\beta), \quad (3.9)$$

$$344 \quad \beta \gg 1, \quad \beta(\theta_b - 1) = O(1) : \quad \frac{\partial \theta}{\partial z} \Big|_{z=0^+} = -q \exp \left[\frac{\beta}{2} (\theta_b - 1) \right] + O(1/\beta), \quad (3.10)$$

$$345 \quad \frac{\partial \theta}{\partial z} \Big|_{z=0^-} = \frac{\partial \theta}{\partial z} \Big|_{z=0^+} - q \frac{\partial Y}{\partial z} \Big|_{z=0^+} + O(1/\beta^2), \quad (3.11)$$

346 $z = 0^+$ and $z = 0^-$ denoting respectively the preheated zone side of the reaction zone and
 347 the exit on the burned-gas side. Equation (3.10) is valid to order unity while (3.11) is valid
 348 up to first order $1/\beta \ll 1$ (included). The back-flow of burned gas is applied on the reaction
 349 sheet so that a boundary condition concerning the flow velocity is added

$$350 \quad z = 0 \quad \tau > 0 : \quad v = v_b(\tau) \quad (3.12)$$

$$351 \quad \tau \leq 0 : \quad v = v_b(0) = S_i, \quad (3.13)$$

352 To leading order in the limit $\beta \gg 1$, the variation of flame temperature is retained in the
 353 Arrhenius factor of (2.10) only. Therefore, when the inner flame structure is in steady state

354 (denoted by an overbar), the laminar flame velocity is,

$$355 \quad \beta \gg 1, \quad \beta(\bar{\theta}_b - 1) = O(1) : \quad \bar{U}_b(T_b)/U_{ref} = \bar{m} = \exp \left[\beta \left(\bar{\theta}_b - 1 \right) / 2 \right] + O(1/\beta) \quad (3.14)$$

356 where $\bar{\theta}_b(\tau) = \theta_u(\tau) + q$ is the flame temperature and $\theta_u(\tau) = T_u(\tau)/T_{ref}$ the instantaneous
357 temperature of unburned gas just ahead of the flame. The instantaneous back-flow (3.4),
358 written in non-dimensional form, then yields

$$359 \quad \bar{v}_b(\tau) = S(\tau)\bar{m} = [1 + \epsilon\tau]S_i \exp \left(\beta [\theta_u(\tau) + q - 1] / 2 \right), \quad (3.15)$$

360 and the delayed back-flow model (3.7) reads

$$361 \quad \beta \gg 1, \quad \tau \geq 0 : \quad v_b(\tau) = \bar{v}_b(\tau) \left[1 - (\beta/2) \frac{\Delta t_w}{t_{ref}} \frac{d\theta_u}{d\tau} \right], \quad \Delta t_w \approx \frac{L}{2a}. \quad (3.16)$$

362 When the unsteadiness of the inner structure of the flame (studied in § 7) is taken into
363 account, the mass flux \bar{m} in (3.16) is replaced by its unsteady version $m(\tau) = \bar{m} + \delta m$,
364 $\bar{v}_b = S(\tau)\bar{m} \rightarrow S(\tau)m(\tau)$, the reduced back flow including the two unsteady effects (in the
365 burned gas and in the inner flame structure) takes the form,

$$366 \quad \beta \gg 1, \quad \tau \geq 0 : \quad v_b(\tau) = S(\tau)e^{\beta[\bar{\theta}_b(\tau)-1]/2} \left[1 + \frac{\delta m(\tau)}{\bar{m}(\tau)} \right] \left[1 - (\beta/2) \frac{\Delta t_w}{t_{ref}} \frac{d\theta_u}{d\tau} \right] \quad (3.17)$$

367 $\delta m(\tau)$ being computed preliminary by the unsteady analysis of the inner structure.

368

3.3. Initial condition

369 Before the elongation starts to increase, the initial condition is a self-similar solution (constant
370 elongation, steady flame structure, $\theta_b(0) = 1$) with a constant back-flow (3.13) $v_b(0) = S_i$
371 and a uniform flow ahead of the flame $\theta = 1 - q$, $v = v_b(0) + q$, the lead shock far ahead from
372 the flame front being considered at infinity. The problem being hyperbolic in the unburned
373 gas outside the flame structure, the downstream boundary condition far away from the flame
374 for solving the unsteady problem is given by the the initial solution,

$$375 \quad z \rightarrow \infty : \quad \pi \approx 1 + O(\epsilon^2), \quad Y = 0, \quad \theta = 1 - q + O(\epsilon^2), \\ 376 \quad v = S_i + q + O(\epsilon^2). \quad (3.18)$$

377 The neglected terms are of the same order of magnitude as the pressure jump across a laminar
378 flame $\delta p/p = O(\epsilon^2)$, according to the steady-state version of (2.29).

379 4. Asymptotic method

380 The problem is solved in the double limit of large activation energy $\beta \gg 1$ and small Mach
381 number of the laminar flame $\epsilon \ll 1$. A first quick look to the compressible flow of unburned
382 gas ahead of the accelerating flame enlightens the multiple length-scale problem.

383

4.1. Preliminary insights into the unburned gas flow ahead of the flame

384 When the flame accelerates the flame acts a semi-transparent piston so that simple com-
385 pression waves are sent in the unburned gas. The dissipative mechanisms being negligible
386 in this external flow, the entropy wave (2.32) propagates from right to left in the reference
387 frame attached to the flame since the flame runs from left to right faster than the flow in
388 the laboratory frame, $m(\tau) > 0$. Therefore, as long as no new shock wave is formed on the
389 leading edge of the compression wave, the entropy is constant ahead of the flame and equal to

390 the downstream entropy ($z \rightarrow \infty$). The isentropic condition $\pi = \theta^{\gamma/(\gamma-1)}$ for small pressure
 391 variations, $\theta = \theta_i(z) + \delta\theta$, $\pi = 1 + \delta\pi$, $\lim_{z \rightarrow \infty} \theta_i = 1 - q$, yields,

$$392 \quad \delta\pi \ll 1 : \quad \delta\theta/\theta_i(z) = [(\gamma - 1)/\gamma]\delta\pi, \quad (4.1)$$

393 the subscript i denoting the initial unperturbed flow $\tau = 0 : \pi_i = 1$. Anyway, in the limit of
 394 small Mach number of the laminar flame $\varepsilon \ll 1$, the shocks that could be produced by the
 395 accelerating flame are weak so that the small entropy jump across the shock is of order of
 396 magnitude ε^3 and thus is negligible when the analysis is limited to ε -term. Then, according
 397 to continuity (2.28),

$$398 \quad \delta\pi = O(\varepsilon), \quad z \gg 1 : \quad \frac{\partial v}{\partial z} = \left[\frac{\partial}{\partial \tau} - m(\tau) \frac{\partial}{\partial z} \right] [\delta\theta - \theta_i \delta\pi] = -\theta_i \frac{1}{\gamma} \left[\frac{\partial}{\partial \tau} - m(\tau) \frac{\partial}{\partial z} \right] \delta\pi. \quad (4.2)$$

399 The viscosity being negligible ahead of the flame, equation (2.29) yields

$$400 \quad \delta\pi \ll 1 : \quad \left[\frac{\partial}{\partial \tau} - m(\tau) \frac{\partial}{\partial z} \right] v = -\frac{1}{\gamma \varepsilon^2} \frac{\partial \delta\pi}{\partial z} \quad (4.3)$$

401 The flow $v(z, \tau)$ can be eliminated from (4.2) and (4.3) to give in the linear approximation

$$402 \quad \frac{(1-q)}{\pi^2} \left[\frac{\partial}{\partial \tau} - m(\tau) \frac{\partial}{\partial z} \right]^2 \delta\pi = \frac{1}{\varepsilon^2} \frac{\partial^2 \delta\pi}{\partial z^2} \delta\pi. \quad (4.4)$$

403 Therefore, considering a time scale of order of the transit time of fluid particles across the
 404 flame, $\partial/\partial\tau = O(1)$, the pressure varies in space with a length scale larger than the flame
 405 thickness by a factor of order $1/\varepsilon$,

$$406 \quad \frac{\partial \delta\pi / \partial z}{\partial \delta\pi / \partial \tau} = O(\varepsilon). \quad (4.5)$$

407 The unsteady term of (4.4) balances the second derivative with respect to space on the right-
 408 hand side since the term $[m\partial\pi/\partial z]$ is negligible in front of $[(1/\varepsilon)\partial\pi/\partial z]$ for $m = O(1)$.
 409 Therefore, the pressure fluctuation satisfies the linear wave equation

$$410 \quad \varepsilon \ll 1 : \quad \frac{\partial^2 \delta\pi}{\partial \tau^2} = \frac{(1-q)}{\varepsilon^2} \frac{\partial^2 \delta\pi}{\partial z^2}; \quad a^2 = \theta a_{\text{ref}}^2 \Rightarrow \frac{\partial^2 \delta\pi}{\partial t^2} \approx a_i^2 \frac{\partial^2 \delta\pi}{\partial x^2}, \quad (4.6)$$

411 written in the original variables using (2.12) and (2.22). Therefore, in the limit $\varepsilon \ll 1$, the
 412 external flow of unburned gas ahead of the flame is governed by the linear acoustics with a
 413 negligible Doppler effect $m(\partial\delta\pi/\partial z)/(\partial\delta\pi/\partial\tau) = O(\varepsilon)$ leading to the scalings

$$414 \quad \tau = O(1) \Rightarrow \varepsilon z = O(1). \quad (4.7)$$

415 According to the continuity equation (4.2), $\partial v/\partial z$ is of order $\partial\delta\pi/\partial\tau$. Anticipating that the
 416 change in flow velocity is of order S_i times the laminar flame velocity $\delta v = O(S_i)$, δv and the
 417 pressure varie on the large length scale $\partial v/\partial z = O(\varepsilon S_i)$, the variation of the non-dimensional
 418 pressure $\delta\pi$ in the external zone is of order εS_i . In the external zone ahead of the flame, the
 419 pressure takes the form

$$420 \quad \pi = 1 + \varepsilon \pi_1(\varepsilon z, \tau), \quad \pi_1 = O(S_i). \quad (4.8)$$

421 The nonlinear solution of the compression wave obtained by Clavin & Champion (2022)
 422 confirms that the limit $\varepsilon \ll 1$ leads to the linear wave (4.6)-(4.8).

423 4.2. Distinguished limit

424 According to (4.8), the spatial variation of pressure in the external flow $\delta\pi = \varepsilon \pi_1 = O(\varepsilon S_i)$,
 425 is larger than in the inner structure of the flame by a factor $1/\varepsilon$ since $\pi_u - \pi_b = \gamma \varepsilon^2 (v_u - v_b) m$

426 where the subscript u denotes the unburned state just ahead of the flame. Neglecting terms of
 427 order ε^2 , the pressure is treated as uniform inside the preheated zone of the flame structure
 428 $z = O(1) : 1 - \pi = O(\varepsilon^2)$. This is also the case in the thin reaction zone $z = O(1/\beta)$ across
 429 which the gradient of the flow velocity varies of order unity so that, according to (2.29),
 430 $\partial^2 v / \partial z^2 \approx (\partial \pi / \partial z) / \gamma \varepsilon^2 \Rightarrow \partial v / \partial z|_{0^-}^{0^+} \approx \pi|_{0^-}^{0^+} / \gamma \varepsilon^2 = O(1) \Rightarrow \pi|_{0^-}^{0^+} = O(\varepsilon^2)$. According
 431 to (3.14) in the limit of large activation energy $\beta \gg 1$, the compressional heating (4.1)
 432 influences the laminar flame velocity and the flame structure as soon as the compression-
 433 induced increase of the flame temperature is of the same order of magnitude as the inverse
 434 of the activation energy $(\gamma - 1) \delta \pi = O(1/\beta) \Rightarrow (\gamma - 1) \varepsilon \delta S_i = O(1/\beta)$. Therefore, as in
 435 the previous analysis of Clavin (2022), the distinguished limit to be considered in the DDT
 436 study is similar to that in Deshaies & Joulin (1989)

$$437 \quad \varepsilon \rightarrow 0, \quad \beta \rightarrow \infty : \quad (\gamma - 1) \beta \varepsilon S_i = O(1). \quad (4.9)$$

438 The comparison with the Zeldovich-Frank-Kamatskii expression (2.8) of ε yields the order
 439 of magnitude of S_i , typically between 5 and 10.

440 4.3. Equations in the limit $\varepsilon \ll 1$

441 According to (4.8), the pressure disturbance is small and varies in space on the rescaled
 442 coordinate $z_1 \equiv \varepsilon z = O(1)$

$$443 \quad \partial \pi / \partial z = O(\varepsilon^2 S_i), \quad \pi = 1 + \varepsilon \pi_1(z_1, \tau), \quad \pi_1 = O(S_i), \quad z_1 \equiv \varepsilon z. \quad (4.10)$$

444 Outside the thin reaction sheet, neglecting second order terms $O(\varepsilon^2)$, equations (2.28)-(2.31)
 445 take the form

$$446 \quad \pi = 1 + \varepsilon \pi_1 : \quad \frac{\partial v}{\partial z} = \left[\frac{\partial}{\partial \tau} - m(\tau) \frac{\partial}{\partial z} \right] \frac{\theta}{1 + \varepsilon \pi_1}, \quad (4.11)$$

$$447 \quad \varepsilon \ll 1 : \quad \frac{\partial v}{\partial z} = [1 - \varepsilon \pi_1] \left[\frac{\partial}{\partial \tau} - m(\tau) \frac{\partial}{\partial z} \right] \theta - \varepsilon \theta \left[\frac{\partial \pi_1}{\partial \tau} - m(\tau) \frac{\partial \pi_1}{\partial z} \right] + O(\varepsilon^2),$$

$$448 \quad \left[\frac{\partial v}{\partial \tau} - m(\tau) \frac{\partial v}{\partial z} - \frac{\partial^2 v}{\partial z^2} \right] = -\frac{1}{\gamma} \frac{1}{\varepsilon} \frac{\partial \pi_1}{\partial z} \quad (4.12)$$

$$449 \quad \left[\frac{\partial Y}{\partial \tau} - m(\tau) \frac{\partial Y}{\partial z} - \frac{\partial^2 Y}{\partial z^2} \right] = 0, \quad Y(z, \tau) \in [0, 1] \quad (4.13)$$

$$450 \quad \left[\frac{\partial \theta}{\partial \tau} - m(\tau) \frac{\partial \theta}{\partial z} - \frac{\partial^2 \theta}{\partial z^2} \right] = \varepsilon \frac{(\gamma - 1)}{\gamma} \theta \left[\frac{\partial \pi_1}{\partial \tau} - m(\tau) \frac{\partial \pi_1}{\partial z} \right] + O(\varepsilon^2). \quad (4.14)$$

451 Equation (4.14) shows how the effect of compressional heating in the unburned gas outside
 452 the flame thickness ($z \gg 1$: $[1/\theta] \partial \theta / \partial \tau = \varepsilon [(\gamma - 1)/\gamma] \partial \pi_1 / \partial \tau$) is transmitted to the
 453 reaction sheet ($z = 0$) by the entropy wave, as it is modified by the heat conduction inside
 454 the preheated zone (second derivative on the left-hand side). According to (4.10), the terms
 455 involving $\partial \pi_1 / \partial z = O(\varepsilon)$ in (4.11) and (4.14) are negligible in the inner structure of the
 456 flame (of order ε^2)

$$457 \quad \frac{\partial v}{\partial z} = [1 - \varepsilon \pi_1] \left[\frac{\partial}{\partial \tau} - m(\tau) \frac{\partial}{\partial z} \right] \theta - \varepsilon \theta \frac{\partial \pi_1}{\partial \tau} + O(\varepsilon^2), \quad (4.15)$$

$$458 \quad \left[\frac{\partial \theta}{\partial \tau} - m(\tau) \frac{\partial \theta}{\partial z} - \frac{\partial^2 \theta}{\partial z^2} \right] = \varepsilon \frac{(\gamma - 1)}{\gamma} \theta \frac{\partial \pi_1}{\partial \tau} + O(\varepsilon^2). \quad (4.16)$$

459 Introducing (4.16) into (4.15), the flow gradient inside the flame structure is expressed in
460 terms of the heat flux and the time-derivative of the pressure

$$461 \quad \frac{\partial v}{\partial z} = [1 - \varepsilon\pi_1] \frac{\partial^2 \theta}{\partial z^2} - \varepsilon \frac{1}{\gamma} \theta \frac{\partial \pi_1}{\partial \tau} + O(\varepsilon^2). \quad (4.17)$$

462 To summarize, in the distinguished limit (4.9), the problem consists in solving (4.12)-(4.13)
463 and (4.16)-(4.17) with the jump conditions (3.9)-(3.15) on the reaction sheet and the boundary
464 conditions (3.18) at infinity.

465 In the present article, the problem is solved analytically in the frame attached to the reaction
466 sheet by an asymptotic method. The corresponding one-dimensional numerical analysis to
467 be performed later for the purpose of comparison is not straightforward. Solving the basic
468 equations for a reaction rate given $W(Y, T)$ as an initial value problem would require to apply
469 a boundary condition at the exit of the moving reaction zone, which is not so usual, see the
470 text below (7.16).

471 5. Matching conditions. Flow in the unsteady flame structure

472 5.1. Back to the external flow ahead of the flame

Denoting the external flow ahead of the flame by the subscript ext_+ the initial condition takes
the form

$$\tau = 0 : \quad \theta_{ext_+} = 1 - q, \quad v_{ext_+} = S_i + q, \quad \pi = 1, \quad (\pi_1 = 0).$$

473 Using the rescaled coordinate $z_1 = \varepsilon z$ in (4.10), equations (4.1) and (4.8) yield

$$474 \quad \theta_{ext_+}(z_1, \tau) = (1 - q) \left[1 + \varepsilon \frac{\gamma - 1}{\gamma} \pi_1(z_1, \tau) \right] + O(\varepsilon^2). \quad (5.1)$$

475 and equation (4.17) takes the form

$$476 \quad \frac{\partial v_{ext_+}}{\partial z} = [1 - \varepsilon\pi_1] \left[\frac{\partial}{\partial \tau} - m(\tau) \frac{\partial}{\partial z} \right] \theta_{ext_+} - \varepsilon \theta_{ext_+} \frac{\partial \pi_1}{\partial \tau} + O(\varepsilon^2)$$

477 yielding
$$\frac{\partial v_{ext_+}(z_1, \tau)}{\partial z_1} = -(1 - q) \frac{1}{\gamma} \frac{\partial \pi_1(z_1, \tau)}{\partial \tau} + O(\varepsilon). \quad (5.2)$$

478 Combined with the leading order of (4.12) in the external flow

$$479 \quad \frac{\partial v_{ext_+}(z, \tau)}{\partial \tau} = -\frac{1}{\gamma} \frac{\partial \pi_1(z_1, \tau)}{\partial z_1} + O(\varepsilon), \quad (5.3)$$

480 the derivative of (5.2) with respect to τ , after elimination of v_{ext_+} , leads to the wave equation
481 (4.6) for the pressure

$$482 \quad \varepsilon \ll 1 : \quad \frac{\partial^2 \pi_1(z_1, \tau)}{\partial \tau^2} = \frac{1}{1 - q} \frac{\partial^2 \pi_1(z_1, \tau)}{\partial z_1^2} + O(\varepsilon) \quad (5.4)$$

where, in the mass-weighted coordinates, the non-dimensional sound speed in the external
zone is $1/\sqrt{1 - q}$. This is easily confirmed as follows

$$z_1 = \varepsilon z = [U_{\text{ref}}/a_{\text{ref}}][\rho/\rho_{\text{ref}}]x/[U_{\text{ref}}t_{\text{ref}}],$$

483 using $\tau = t/t_{\text{ref}}$, the ratio z_1/τ takes the form $z_1/\tau = [x/at]\rho a/[\rho_{\text{ref}}a_{\text{ref}}]$ to give, using
484 $\rho a/[\rho_{\text{ref}}a_{\text{ref}}] = [p/p_{\text{ref}}]\sqrt{T_{\text{ref}}/T}$, $(z_1/\tau) = [(x/at)/\sqrt{\theta}][1 + O(\varepsilon)]$ with, according to (5.1),
485 $\theta = 1 - q + O(\varepsilon)$.

486 The flow of unburned gas being uniform and steady far ahead from the flame, the external

487 flow is a downstream-running compression wave (propagating in the same direction as the
 488 flame) with a leading edge in the form of a weak singularity propagating with the sound speed
 489 relative to the flow. Then, according to (5.4), $\pi_1(z_1, \tau)$ and $v_{ext_+}(z_1, \tau) = S_i + q + \delta v_{ext_+}(z_1, \tau)$
 490 are functions of a single variable $\tau - \sqrt{1-q} z_1$

$$491 \quad z_1 \leq \tau / \sqrt{1-q} : \quad \pi_1 = \pi_u(\tau - \sqrt{1-q} z_1), \quad \delta v_{ext_+} = \Phi(\tau - \sqrt{1-q} z_1), \quad (5.5)$$

$$492 \quad \text{with} \quad \pi_u(\tau) \equiv \pi_1|_{z_1=0}, \quad \pi_u(0) = 0, \quad \Phi(\tau) \equiv \delta v_{ext_+}|_{z_1=0}, \quad \Phi(0) = 0$$

493 so that the quasi-uniform pressure in the flame structure is $1 + \varepsilon \pi_u(\tau)$. Using (5.5) in the
 494 form $\partial v_{ext_+} / \partial z_1 = -\sqrt{1-q} \partial v_{ext_+} / \partial \tau$, equation (5.3) yields

$$495 \quad \frac{\partial v_{ext_+}}{\partial z_1} = \frac{\sqrt{1-q}}{\gamma} \frac{\partial \pi_1}{\partial z_1} + O(\varepsilon). \quad (5.6)$$

496 in agreement the linear relation $\delta p \approx \bar{\rho} \bar{a} \delta u$ of an acoustic wave propagating from left to
 497 right. The flow field $v_{ext_+}(z_1, \tau)$ is obtained by integrating (5.6) from the leading edge of the
 498 compression wave where, to leading order, the boundary conditions (3.18) $v_{ext_+} = S_i + q$
 499 and $\pi_1 = 0$ hold

$$500 \quad v_{ext_+}(z_1, \tau) - (S_i + q) = \frac{\sqrt{1-q}}{\gamma} \pi_1(z_1, \tau) + O(\varepsilon), \quad \delta v_{ext_+} \approx \frac{\sqrt{1-q}}{\gamma} \pi_1(z_1, \tau). \quad (5.7)$$

501 According to (5.5) and (5.7), the relation linking the flow to the pressure just ahead of the
 502 flame ($z_1 = 0$) takes the form

$$503 \quad v_{ext_+}(z_1 = 0, \tau) = S_i + q + \frac{\sqrt{1-q}}{\gamma} \pi_u(\tau) + O(\varepsilon) \quad (5.8)$$

$$504 \quad \frac{\partial \pi_1}{\partial z_1} \Big|_{z_1=0} = -\sqrt{1-q} \frac{d\pi_u(\tau)}{d\tau} \Rightarrow \frac{\partial v_{ext_+}}{\partial z_1} \Big|_{z_1=0} = -\frac{(1-q)}{\gamma} \frac{d\pi_u(\tau)}{d\tau} + O(\varepsilon) \quad (5.9)$$

505 in agreement with (5.2). These relations are useful for matching the flow of the inner structure
 506 with the external flow of unburned gas in § 5.3.

507 *5.2. Matching the temperature*

508 From now on, the superscript (i) denotes the solution in the preheated zone of the flame
 509 structure ($z > 0$). Inside the flame structure, the spatial variation of pressure introduces a
 510 negligible term of order ε^2 so that $\partial \pi_1 / \partial \tau$ in (4.16)-(4.17) can be replaced by the function
 511 $d\pi_u(\tau) / d\tau \equiv \partial \pi_1 / \partial \tau|_{z_1=0}$ describing the coupling of the flame structure with the external
 512 solution on the cold gas. Therefore, (4.16) can be written as

$$513 \quad z \geq 0 : \quad \left[\frac{\partial \theta^{(i)}}{\partial \tau} - m(\tau) \frac{\partial \theta^{(i)}}{\partial z} - \frac{\partial^2 \theta^{(i)}}{\partial z^2} \right] = \varepsilon \frac{(\gamma-1)}{\gamma} \theta^{(i)}(z, \tau) \frac{d\pi_u(\tau)}{d\tau} + O(\varepsilon^2) \quad (5.10)$$

514 where $\pi_u(\tau) \equiv \pi_1|_{z_1=0}$. The boundary condition at infinity on the cold gas side of the
 515 preheated zone ($z = O(1)$, $z \rightarrow \infty$) is obtained by matching the preheated zone $\theta^{(i)}(z, \tau)$ and
 516 the external flow $\theta_{ext_+}(z_1, \tau)$

$$517 \quad \lim_{z \rightarrow \infty} \theta^{(i)}(z, \tau) = \theta_{ext_+}(z_1, \tau)|_{z_1=0}, \quad \lim_{z \rightarrow \infty} \partial \theta^{(i)} / \partial z = \varepsilon \partial \theta_{ext_+} / \partial z_1|_{z_1=0} = O(\varepsilon^2),$$

518 where, according to (5.1) $\theta_{ext_+} = (1-q) + \varepsilon(1-q)[(\gamma-1)/\gamma] \pi_1(z_1, \tau) + O(\varepsilon^2)$, $\partial \theta_{ext_+} / \partial z_1 =$
 519 $O(\varepsilon)$ so that $\lim_{z \rightarrow \infty} \partial \theta^{(i)} / \partial z = O(\varepsilon^2)$ is negligible to first order in a perturbation analysis

520 for small ε ,

$$521 \quad \lim_{z \rightarrow \infty} \theta^{(i)}(z, \tau) - (1 - q) \approx \varepsilon(1 - q) \frac{\gamma - 1}{\gamma} \pi_u(\tau), \quad \lim_{z \rightarrow \infty} \partial \theta^{(i)} / \partial z \approx 0. \quad (5.11)$$

522 Equations (4.13) and (5.10) have to be solved using (5.11) and the boundary conditions (3.9)-
523 (3.11) on the reaction sheet ($z = 0$) in the distinguished limit (4.9). Equation (3.10) involves
524 the flame temperature $\theta_b(\tau) - 1 \equiv \theta^{(i)}(z, \tau)|_{z=0} - 1 = O(1/\beta)$ which is a time-dependent
525 eigenvalue of the problem, obtained by the jump condition (3.11). In the fully unsteady
526 problem, the solution in the burned gas side of the reaction sheet $z < 0$ is required in (3.11).
527 We will come back to this question later.

528 5.3. Matching the flow velocity

529 Matching the flow velocity in the preheated zone with the external flow of cold gas yields

$$530 \quad \lim_{z \rightarrow \infty} v^{(i)}(z, \tau) = v_{ext_+}(z_1, \tau)|_{z_1=0} = S_i + q + \frac{\sqrt{1 - q}}{\gamma} \pi_u(\tau) + O(\varepsilon), \quad (5.12)$$

$$531 \quad \lim_{z \rightarrow \infty} \frac{\partial v^{(i)}}{\partial z} = \varepsilon \frac{\partial v_{ext_+}}{\partial z_1} \Big|_{z_1=0} = -\varepsilon \frac{(1 - q)}{\gamma} \frac{d\pi_u(\tau)}{d\tau} + O(\varepsilon^2) \quad (5.13)$$

532 where (5.8)-(5.9) have been used. Equations (5.12)-(5.13) yield

$$533 \quad \lim_{z \rightarrow \infty} v^{(i)}(z, \tau) \rightarrow S_i + q + \frac{\sqrt{1 - q}}{\gamma} \pi_u(\tau) - \varepsilon z \frac{(1 - q)}{\gamma} \frac{d\pi_u(\tau)}{d\tau} + O(\varepsilon^2). \quad (5.14)$$

Integration of (4.17), written in the preheated zone in the form

$$\frac{\partial v^{(i)}}{\partial z} = \left[1 - \varepsilon \pi_u(\tau) \right] \frac{\partial^2 \theta^{(i)}}{\partial z^2} - \varepsilon \frac{1}{\gamma} \left[\theta^{(i)} - (1 - q) \right] \frac{d\pi_u(\tau)}{d\tau} - \varepsilon(1 - q) \frac{1}{\gamma} \frac{d\pi_u(\tau)}{d\tau} + O(\varepsilon^2)$$

534 from the reaction sheet $z = 0$: $v^{(i)} = v_b(\tau)$ yields

$$535 \quad z = O(1) : \quad v^{(i)}(z, \tau) - v_b(\tau) = [1 - \varepsilon \pi_u(\tau)] \left(\frac{\partial \theta^{(i)}}{\partial z} - \frac{\partial \theta^{(i)}}{\partial z} \Big|_{z=0^+} \right) \quad (5.15)$$

$$536 \quad -\varepsilon \frac{1}{\gamma} \frac{d\pi_u(\tau)}{d\tau} \int_0^z [\theta^{(i)} - (1 - q)] dz - \varepsilon z (1 - q) \frac{1}{\gamma} \frac{d\pi_u(\tau)}{d\tau} + O(\varepsilon^2).$$

537 Thanks to (5.11) $\lim_{z \rightarrow \infty} \theta^{(i)}(z, \tau) = (1 - q) + O(\varepsilon)$, the leading order of the integral on the
538 right-hand side of (5.15) is well defined in the limit $z \rightarrow \infty$ and is of order unity. Then, using
539 (5.14), the limit $z \rightarrow \infty$ of (5.15) yields

$$540 \quad v_b(\tau) - \left[S_i + q + \frac{\sqrt{1 - q}}{\gamma} \pi_u(\tau) \right] =$$

$$541 \quad [1 - \varepsilon \pi_u(\tau)] \frac{\partial \theta^{(i)}}{\partial z} \Big|_{z=0^+} + \varepsilon \frac{1}{\gamma} \frac{d\pi_u(\tau)}{d\tau} \int_0^{+\infty} [\theta^{(i)} - (1 - q)] dz + O(\varepsilon^2). \quad (5.16)$$

542 where the thermal flux out of the reaction sheet $\partial \theta^{(i)} / \partial z|_{z=0^+}$ is obtained in terms of the
543 flame temperature θ_b by the jump condition (3.10). The integral term on the right-hand side
544 of (5.16) is meaningful as soon as $d\pi_u(\tau)/d\tau < \varepsilon$.

5.4. Master equation

545

546 Using the jump relation (3.10), equation (5.16) yields

$$547 \quad v_b(\tau) - \left[S_i + q + \frac{\sqrt{1-q}}{\gamma} \pi_u(\tau) \right] \quad (5.17)$$

$$548 \quad = -q [1 - \varepsilon \pi_u(\tau)] \exp \left[\frac{\beta}{2} (\theta_b - 1) \right] + \varepsilon \frac{1}{\gamma} \frac{d\pi_u(\tau)}{d\tau} \int_0^{+\infty} [\theta^{(i)} - (1-q)] dz + O(\varepsilon^2).$$

549 Anticipating that $\beta(\theta_b - 1)$ is of order unity in the distinguished limit (4.9) and neglecting ε
550 terms, equation (5.17) gives a general equation of order unity, called the master equation

$$551 \quad v_b(\tau) - \left[S_i + q + \frac{\sqrt{1-q}}{\gamma} \pi_u(\tau) \right] = -q \exp \left(\frac{\beta}{2} [\theta_b(\tau) - 1] \right) + O(\varepsilon). \quad (5.18)$$

552 This equation is valid for the ZFK model of flames even if the inner structure is unsteady.
553 Under the quasi-steady approximation, equation (5.18) can be obtained more directly by the
554 conservation of mass across the flame $\bar{U}_b/\bar{U}_L = \bar{T}_b/T_u$ combined with the relation between
555 the laminar flame velocities \bar{U}_b and \bar{U}_L and the flows in the unburned mixture ahead of the
556 flame u_u and in the burned gas \bar{u}_b , $u_u - \bar{u}_b = \bar{U}_b - \bar{U}_L = [(\bar{T}_b - T_u)/\bar{T}_b] \bar{U}_b$. The latter
557 expression takes the form $u_u - \bar{u}_b = q \bar{U}_b [1 + O(1/\beta)]$ in the limit of large activation energy,
558 the relative variation of the flame temperature $\bar{T}_b(\tau)/\bar{T}_b(0) - 1$ being of order $1/\beta$. Using
559 (5.12) $u_u(\tau) = S_i + q + [\sqrt{1-q}/\gamma] \pi_u(\tau)$ and (2.9) $\bar{U}_b \approx U_b(0) e^{\beta(\bar{\theta}_b - 1)/2}$, equation (5.18) is
560 recovered. Although the laminar flame velocity \bar{U}_b (2.9) is no longer valid for an unsteady
561 flame structure, equation (5.18) is still valid when the unsteady flame temperature $\theta_b(\tau)$
562 computed from the unsteady flame structure is used on the right-hand side.

563 **6. Pressure and flame temperature runaway.**

564 In this section the inner structure of the flame is assumed in steady state. The essential
565 mechanism of the pressure runaway is more easily revealed under this approximation. The
566 latter is removed in section § 7 leading to the same phenomenology as in § 6.3.

567

6.1. Quasi-steady inner structure.

568 If the inner structure of the flame is in steady state (denoted by an overbar), the terms $\partial\theta^{(i)}/\partial\tau$
569 and $\varepsilon d\pi_u(\tau)/d\tau$ are neglected in (5.10) leading to

$$570 \quad z \geq 0 : \bar{Y} = e^{-\bar{m}z}, \quad \bar{\theta}^{(i)}(z, \tau) = \left[\bar{\theta}_b - \theta_u \right] e^{-\bar{m}z} + \theta_u,$$

$$571 \quad z \leq 0 : \bar{Y} = 1, \quad \bar{\theta}^{(i)} = \bar{\theta}_b(\tau) \quad (6.1)$$

572 where the short notation

$$573 \quad \theta_u(\tau) \equiv (1-q) \left[1 + \varepsilon \frac{\gamma-1}{\gamma} \pi_u(\tau) \right], \quad (6.2)$$

574 has been introduced for the gas temperature just ahead of the flame as it is modified by the
575 downstream-running acoustic wave in the unburned gas, see (5.11). Introducing the parameter
576 b of order unity in the distinguished limit (4.9)

$$577 \quad b \equiv \frac{\beta\varepsilon}{2} (1-q) \frac{(\gamma-1)}{\gamma}, \quad \varepsilon \rightarrow 0, \quad \beta \rightarrow \infty : \quad bS_i = O(1), \quad (6.3)$$

578 the jump conditions across the reaction sheet (3.10)-(3.11) yield

$$579 \quad \bar{\theta}_b(\tau) = \theta_u + q, \quad \bar{\theta}_b - 1 = \varepsilon(1 - q) \frac{\gamma - 1}{\gamma} \pi_u + O(\varepsilon^2), \quad (6.4)$$

$$580 \quad \beta(\bar{\theta}_b - 1)/2 = \beta[\theta_u + q - 1]/2 = b\pi_u, \quad \bar{m} = e^{b\pi_u} + O(1/\beta), \quad (6.5)$$

$$581 \quad \bar{\theta}^{(i)}(z, \tau) = qe^{-\bar{m}z} + (1 - q) \left[1 + \varepsilon \frac{\gamma - 1}{\gamma} \pi_u(\tau) \right]. \quad (6.6)$$

582 **6.2. Back flow.**

583 In the quasi-steady approximation, the back-flow reduces to the instantaneous model (3.15),

$$584 \quad v_b(\tau) = S\bar{m} = S(\tau) e^{b\pi_u(\tau)}. \quad (6.7)$$

585 Introducing (6.7) into the master equation (5.18) yields the same transcendental equation for
586 the flame pressure $\pi_u = \pi_1|_{z_1=0} = [p/p_{\text{ref}}|_{z_1=0} - 1]/\varepsilon = O(1)$ (or the flame temperature) as
587 obtained when the flame is considered as a discontinuity, see Clavin (2022)

$$588 \quad (S + q)e^{b\pi_u} = S_i + q + (\sqrt{1 - q}/\gamma) \pi_u. \quad (6.8)$$

589 **6.2.1. Turning point.**

590 Introducing the notation

$$591 \quad \vartheta \equiv b\pi_u = O(1), \quad \zeta \equiv S + q, \quad \zeta(\tau) = (1 + \varepsilon\tau)S_i + q, \quad (6.9)$$

$$592 \quad \tilde{b} \equiv b\gamma/\sqrt{1 - q} = (\beta\varepsilon/2)(\gamma - 1)\sqrt{1 - q} = O(1/S_i) \quad (6.10)$$

593 equation (6.8) takes the reduced form

$$594 \quad \zeta e^{\vartheta} - \zeta_i - \vartheta/\tilde{b} = 0; \quad \tau = 0: \quad \zeta = \zeta_i \equiv S_i + q, \quad \vartheta = 0. \quad (6.11)$$

595 The solution yields the pressure in terms of the elongation $\vartheta(\zeta)$. The solution depends on the
596 initial elongation ζ_i and involves a single parameter \tilde{b} . Using the elongation versus the time
597 in (3.1) $S(\tau) = [1 + \varepsilon\tau]S_i$, the solution $\vartheta(\zeta)$ provides us with the dynamics of the pressure
598 and/or the flame temperature. The graph of the inverse function $\zeta(\vartheta)$ is a bell-shaped curve
599 sketched in figure 2, the maximum of which corresponds to $\zeta = \zeta^*$ and $\vartheta = \vartheta^*$

$$600 \quad \left. \frac{d\zeta}{d\vartheta} \right|_{\vartheta=\vartheta^*} = 0: \quad \zeta^* e^{\vartheta^*} = \frac{1}{\tilde{b}}, \quad \vartheta^* = 1 - \zeta_i \tilde{b} > 0, \quad \frac{\zeta^*}{\zeta_i} = \frac{e^{[\tilde{b}\zeta_i - 1]}}{\tilde{b}\zeta_i} \geq 1, \quad (6.12)$$

601 the inequality $\zeta^*/\zeta_i \geq 1$ being valid for all the reactive gaseous mixtures ($0 < \tilde{b}\zeta_i \leq 1$),
602 see Clavin (2022). The dynamics of the flame is represented by the C-shaped curve $\vartheta(\zeta)$
603 with a turning point at the critical elongation S^* , $\zeta^* = S^* + q$, $d\vartheta/d\zeta|_{\zeta=\zeta^*} = \infty$. There is
604 no more solution to (6.11) for $\zeta > \zeta^*$. For $\zeta < \zeta^*$, there are two branches of solutions
605 $\bar{\vartheta}_{\pm} = \vartheta^* \pm \sqrt{2(\zeta^* - \zeta)/\zeta^*}$, $\bar{\vartheta}_- - \vartheta^* < 0 < \bar{\vartheta}_+ - \vartheta^*$, $d\bar{\vartheta}_-/d\zeta > 0$ and $d\bar{\vartheta}_+/d\zeta < 0$ for the
606 other, see figure 2. According to the thermodynamics law, the temperature increases during
607 an adiabatic compression so that the physical branch of solutions is $\bar{\vartheta}_-(\zeta)$.

608 As noticed in Clavin (2022), the limiting case $\zeta_i = \zeta^*$, $S = S_{\text{max}}$ corresponds to a
609 universal critical Mach number $u_u^*/a_u^* = 2/[\beta(\gamma - 1)]$ characterizing the pre-conditioned
610 flow of unburned gas just before the DDT onset. This critical Mach number of the cold flow
611 is typically $u_u^*/a_u^* \approx 0.65$ for ordinary flames ($\beta \approx 8$) and becomes slightly supersonic
612 $u_u^*/a_u^* > 1$ for a very energetic mixture ($\beta \lesssim 4$) while the laminar flame velocity remains
613 very subsonic $U_b^*/a_b^* \approx 0.05$, in agreement with the experiments of Kuznetsov *et al.* (2010)
614 and the numerics of Liberman *et al.* (2010) and Ivanov *et al.* (2011).

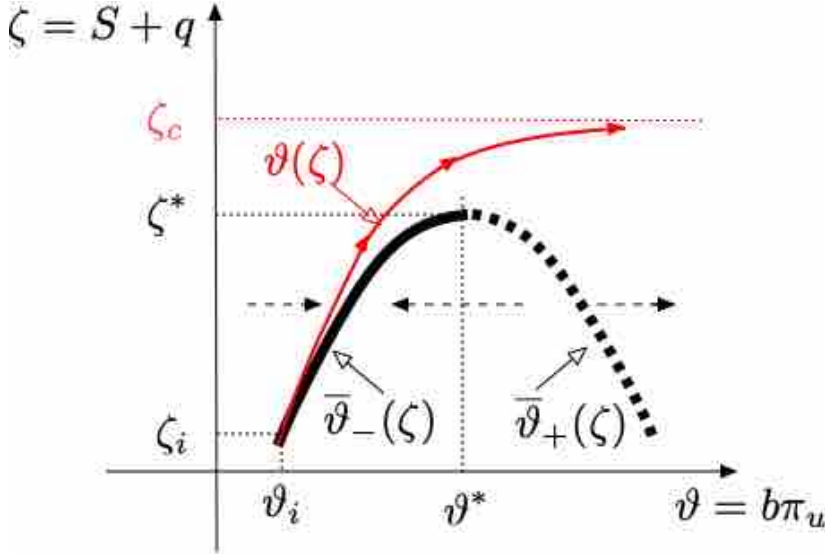


Figure 2: Sketch of the solutions "elongation ζ versus pressure ϑ " (not to scale). The two branches $\bar{\vartheta}_{\pm}(\zeta)$ of solutions of the quasi-steady equation (6.11) in thick line show the critical elongation ζ^* , above which there is no quasi-steady solutions ($\bar{\vartheta}_-$ is the physical solution). The horizontal arrows in broken line indicate the direction of the trajectories of (6.23) for $\bar{\epsilon}_w > 0$ showing the stability of the branch of physical solutions of (6.11), see

Strogatz (1994). They are in the opposite direction for $\bar{\epsilon}_w < 0$. The solution of the dynamical equation (6.23) $\vartheta(\zeta)$ in thin red line shows the finite-time divergence of the pressure at the elongation $\zeta_c > \zeta^*$, $\lim_{(\zeta - \zeta_c) \rightarrow 0^-} \vartheta = \infty$. The red arrows indicate the direction of increasing time for an elongation increasing with the time. According to (6.27), the relative difference in critical elongations is small for a small elongation rate

$$(3.1) \quad \epsilon \ll 1: (\zeta_c - \zeta^*)/\zeta^* = O((\epsilon S_i/\zeta^*)^{2/3}).$$

615 6.2.2. Finite-time singularity of the flow gradient

616 According to (6.12) $d\zeta/d\tau = \epsilon S_i$, the elongation and the flame velocity $\bar{m} = e^{\vartheta}$ ($\vartheta \equiv b\pi_u$)
 617 increase first slowly with the time $d\bar{m}/d\tau = O(\epsilon S_i)$, and, according to (6.12), the flame
 618 acceleration diverges abruptly $d\vartheta/d\zeta|_{\zeta=\zeta^*} = \infty$, $d\bar{m}/d\tau|_{\tau=\tau^*} = \epsilon S_i \bar{m}^* d\vartheta/d\zeta|_{\zeta=\zeta^*} = \infty$ when
 619 the elongation reaches S^* , namely when the flame velocity reaches the critical value $\bar{m}^* = e^{\vartheta^*}$
 620 which is finite ($\vartheta^* < 1$). As in the piston problem considered in Clavin & Tofaili (2021),
 621 equation (6.11) takes a generic form near the critical point $d\zeta/d\vartheta|_{\vartheta=\vartheta^*} = 0$,

$$622 \quad \left. \frac{d^2\zeta}{d\vartheta^2} \right|_{\vartheta=\vartheta^*} = -\zeta^* \quad \Rightarrow \quad \frac{\zeta^* - \zeta}{\zeta^*} \ll 1: \quad \frac{\zeta^* - \zeta}{\zeta^*} \approx \frac{1}{2}(\vartheta^* - \vartheta)^2 \quad (6.13)$$

$$623 \quad \vartheta^* - \vartheta \approx \sqrt{2} \sqrt{\frac{\zeta^* - \zeta}{\zeta^*}}, \quad b(\pi_u^* - \pi_u) \approx \sqrt{\frac{(S^* - S)}{(S^* + q)/2}}, \quad (6.14)$$

624 obtained by a Taylor expansion. The dynamics of flame pressure and flame temperature near
 625 the critical condition at $\tau = \tau^*$ takes the form

$$626 \quad \vartheta^* - \vartheta(\tau) \approx \kappa \sqrt{\tau^* - \tau} \quad \text{where} \quad \kappa \equiv \sqrt{2\epsilon \frac{S_i}{S^* + q}} = O(\sqrt{\epsilon}), \quad (6.15)$$

627 exhibiting the finite-time singularity of the flame acceleration

$$628 \quad \tau/\tau^* - 1 \rightarrow 0_- : \vartheta \rightarrow \vartheta^* = 1 - \zeta_i \tilde{b} > 0, \quad \pi_u \rightarrow \pi_u^* = \vartheta^*/b, \quad \bar{m} \rightarrow \bar{m}^* = e^{\vartheta^*} \quad (6.16)$$

$$629 \quad \frac{d\vartheta}{d\tau} \approx \frac{\kappa/2}{\sqrt{\tau^* - \tau}}, \quad \frac{d\pi_u}{d\tau} \approx \frac{\kappa/2b}{\sqrt{\tau^* - \tau}}, \quad \frac{1}{\bar{m}} \frac{d\bar{m}}{d\tau} \approx \frac{\kappa/2}{\sqrt{\tau^* - \tau}}, \quad (6.17)$$

630 According to (5.2)-(5.9) and (6.15)-(6.17),

$$631 \quad \tau/\tau^* - 1 \rightarrow 0_- : \quad \frac{\partial v_{ext_+}(z_1, \tau)}{\partial z_1} \approx -\frac{(1-q)\kappa/2}{\gamma} \frac{1}{b} \frac{1}{\sqrt{\tau^* - \tau + z_1 \sqrt{1-q}}},$$

$$632 \quad \frac{\partial v_{ext_+}(z_1, \tau)}{\partial \tau} \approx \frac{\sqrt{1-q}\kappa/2}{\gamma} \frac{1}{b} \frac{1}{\sqrt{\tau^* - \tau + z_1 \sqrt{1-q}}}$$

633 the gradient and acceleration of the external unburned flow diverges on the flame,

$$634 \quad \tau \rightarrow \tau^* : \quad \left. \frac{\partial v_{ext_+}}{\partial z_1} \right|_{z_1=0} \approx \frac{(1-q)\kappa/2}{\gamma} \frac{1}{b} \frac{1}{\sqrt{\tau^* - \tau}}, \quad \left. \frac{\partial v_{ext_+}}{\partial \tau} \right|_{z_1=0} \approx \frac{\sqrt{1-q}\kappa/2}{\gamma} \frac{1}{b} \frac{1}{\sqrt{\tau^* - \tau}}.$$

635 This suggests a finite-time singularity of the flow gradient leading to the formation of a shock
636 inside the quasi-isobaric flame structure. The DDT mechanism is associated with an even
637 more violent phenomenon: a catastrophic behavior of the flame structure is predicted below
638 by the delayed back-flow model.

639 6.3. Delayed back-flow model. Catastrophic dynamics.

640 The unsteady flow behind the tip of the elongated flame is a too complex problem for an
641 analytical study. Equation (3.16) is a simplified model for analyzing the main consequence of
642 this unsteadiness, a detailed expression of the delay Δt_w is not useful in the following. Only
643 the order of magnitude of Δt_w matters for a clear understanding of the phenomenon. Still
644 assuming the inner structure of the flame in steady-state $\bar{m} = e^{b\pi_u(\tau)}$, $d\bar{m}/d\tau \approx \bar{m} b d\pi_u/d\tau$
645 the delayed back-flow model (3.16) reads

$$646 \quad v_b = S_i(1 + \epsilon\tau) \bar{m} \left[1 - \frac{\Delta t_w}{t_{ref}} b \frac{d\pi_u}{d\tau} + \dots \right] \quad (6.18)$$

$$647 \quad v_b \approx S_i e^{b\pi_u(\tau)} + \epsilon\tau S_i e^{b\pi_u^*} - S_i e^{b\pi_u^*} \frac{\Delta t_w}{t_{ref}} b \frac{d\pi_u}{d\tau} + \dots \quad (6.19)$$

648 where, considering $\Delta t_w/t_{ref}$ of order unity and $d\pi_u/d\tau$ of order $\epsilon < 1$, the $e^{b\pi_u}$ term in
649 the second and third term on the right-hand side has been considered as constant nearby the
650 turning point for simplicity.

651 6.3.1. Dynamical equation for the pressure and the flame temperature

652 Introducing (6.5) and (6.19) into the master equation equation (5.18) yields an ordinary
653 differential equation (ODE) of first order for $\pi_u(\tau)$

$$654 \quad S_i e^{b\pi_u(\tau)} + \epsilon\tau S_i e^{b\pi_u^*} - S_i e^{b\pi_u^*} \frac{\Delta t_w}{t_{ref}} b \frac{d\pi_u}{d\tau} - \left[S_i + q + \frac{\sqrt{1-q}}{\gamma} \pi_u(\tau) \right] = -q e^{b\pi_u(\tau)}$$

655 which can be written in the form

$$656 \quad [S_i(1 + \epsilon\tau) + q] e^{b\pi_u(\tau)} - \left[S_i + q + \frac{\sqrt{1-q}}{\gamma} \pi_u(\tau) \right] = K_w b \frac{d\pi_u(\tau)}{d\tau}. \quad (6.20)$$

$$657 \quad \text{where } K_w \equiv S_i e^{b\pi_u^*} \frac{\Delta t_w}{t_{ref}} > 0 \quad (6.21)$$

658 Written with the notation (6.10)-(6.11), a nonlinear ODE for $\vartheta(\zeta) = b\pi_u(\zeta)$ is obtained

$$659 \quad \zeta \exp \vartheta - \zeta_i - \vartheta/\tilde{b} = \tilde{K}_w \frac{d\vartheta}{d\zeta}, \quad \text{where } \tilde{K}_w \equiv \epsilon S_i K_w \quad \text{and} \quad \tilde{b} \equiv b\gamma/\sqrt{1-q}. \quad (6.22)$$

660 The roots of the left hand-side of the first equation (6.22) are the quasi-steady solutions (6.11)
661 of the instantaneous back-flow model $\bar{\vartheta}_\pm(\zeta)$ shown in figure 2. Focusing our attention on the
662 vicinity of the turning point, following (6.15), a power expansion in $(\vartheta - \vartheta^*)$ limited to the
663 quadratic terms yields

$$664 \quad \frac{(\zeta - \zeta^*)}{\zeta^*} + \frac{(\vartheta^* - \vartheta)^2}{2} = \tilde{\epsilon}_w \frac{d\vartheta}{d\zeta}, \quad \text{where } \tilde{\epsilon}_w \equiv \tilde{b}\tilde{K}_w = \epsilon \frac{S_i^2 \Delta t_w}{\zeta^* t_{ref}}. \quad (6.23)$$

665 For $\zeta < \zeta^*$, the sign of the left-hand side of (6.23) is positive for $\vartheta < \bar{\vartheta}_-$ and for $\vartheta > \bar{\vartheta}_+$
666 (negative for $\bar{\vartheta}_- < \vartheta < \bar{\vartheta}_+$). The trajectories in the phase space of (6.23) show that the
667 physical branch $\bar{\vartheta}_-(\zeta)$ is stable since $\tilde{\epsilon}_w > 0$. The other branch $\bar{\vartheta}_+(\zeta)$ is unstable. A finite
668 time singularity of the solution of (6.23) occurs around the turning point, as shown now.

669 6.3.2. Dynamical saddle-node bifurcation

670 Equation (6.23) describes the dynamics nearby a saddle-node bifurcation. Such an equation
671 was extensively used for sharp transitions in different problems of physics or biophysics. The
672 theory of catastrophic events based on this equation has been recently revisited and extended
673 by Peters *et al.* (2012). Conveniently rescaled

$$674 \quad (1/2^{2/3})(\zeta^*/\tilde{\epsilon}_w)^{1/3}(\vartheta - \vartheta^*) \rightarrow y', \quad (1/2^{1/3})(\zeta^*/\tilde{\epsilon}_w)^{2/3}(\zeta - \zeta^*)/\zeta^* \rightarrow t' \quad (6.24)$$

675 equation (6.23), after multiplication by $(\zeta^*/\sqrt{2}\tilde{\epsilon}_w)^{2/3}$, takes a generic normal form

$$676 \quad \frac{dy'(t')}{dt'} = t' + y'^2 \quad (6.25)$$

677 with two fixed points for $t' < 0$, the stable one corresponding to the negative root $y' = -\sqrt{-t'}$
678 (physical branch of solutions). The fixed points collapse at $t' = 0$ and there is no more fixed
679 point for $t' > 0$ (saddle-node bifurcation). Considering an initial condition on the stable
680 branch $t' = t'_i < 0 : y' = -\sqrt{-t'_i}$ for $-t'_i/t'_c = y_i'^2/t'_c$ larger than unity, the asymptotic solution
681 of (6.25) is obtained in terms of the Airy function to give

$$682 \quad \lim_{t \rightarrow t'_c} y'(t') = \frac{1}{t'_c - t'} - \frac{t'_c}{3}(t'_c - t') + \dots \quad \text{where } t'_c \approx 2.338\dots, \quad (6.26)$$

683 see the references in Peters *et al.* (2012). The finite-time singularity (6.26) is of the same
684 type as the solution of the Riccati equation $dy'/dt' = y'^2$. According to (6.26), the pressure
685 and the flame temperature $\vartheta \equiv b\pi_u(\tau)$ blow up at time $\tau = \tau_c$ for a finite elongation
686 $\zeta_c = S_i(1 + \epsilon\tau_c) + q$, $(\zeta_c - \zeta^*) = (\tau_c - \tau^*)\epsilon S_i$

$$687 \quad \frac{\zeta_c - \zeta^*}{(2\zeta^* \tilde{\epsilon}_w^2)^{1/3}} = 2.338\dots, \quad b(\pi_u - \pi_u^*) \equiv \vartheta - \vartheta^* \approx \frac{2\tilde{\epsilon}}{\zeta_c - \zeta} = \frac{2b\gamma}{\sqrt{1-q}} \frac{K_w}{\tau_c - \tau}. \quad (6.27)$$

688 The solution to (6.23) increases above the critical elongation $\vartheta(\tau) > \vartheta^*$ and diverges like
 689 $K_w/(\tau_c - \tau)$ where $\tau_c - \tau^* \propto K_w^{2/3}/(\epsilon S_i)^{1/3}$, see figure 2. The smaller the elongation rate $\epsilon < 1$,
 690 the closer to the turning point S^* the pressure blowup, $\lim_{\epsilon \rightarrow 0}(S_c - S^*)/S_i \propto (\epsilon S_i K_w)^{2/3}$.
 691

692 To summarize, unsteadiness of the burned gas flow which is modeled by a delay in the back
 693 flow in § 6.3 has a drastic effect on the dynamics, more drastic than the instantaneous back-
 694 flow in § 6.2: the flame structure is blown off as a whole in finite time when the elongation
 695 increases slowly. A strong increase in pressure and flame temperature occurs abruptly with
 696 a sudden shrinking of the flame thickness for an elongation slightly larger than the critical
 697 elongation of the instantaneous back-flow model.

698 7. Unsteadiness of the flame structure

699 Due to the singularity of the flame acceleration, the quasi-steady approximation of the inner
 700 structure of the flame on the tip is doubtful at the end of the process. The objective of this
 701 section is to get rid of this assumption.

702 7.1. Unsteady inner structure of the flame

703 Introducing the decomposition $w = \bar{w} + \delta w$ where \bar{w} denotes the quasi-steady approximation
 704 of the inner structure, a perturbation analysis of (4.13) and (4.16) is performed in the
 705 distinguished limit (4.9)

$$706 \quad \epsilon \ll \epsilon \ll 1, \quad d\pi_u/d\tau = O(\epsilon), \quad \beta \gg 1, \quad (\gamma - 1)\beta \epsilon S_i = O(1) \quad (7.1)$$

707 retaining unsteady terms of order $\epsilon d\pi_u/d\tau = O(\epsilon\epsilon)$ in these equation and neglecting smaller
 708 terms, namely those of order $\epsilon(d\pi_u/d\tau)^2$ and ϵ^2 . The first order terms are sufficient to draw
 709 a final conclusion concerning the finite-time singularity.

710 7.1.1. Preheated zone ($z \geq 0$)

711 Anticipating that $\beta(\theta_b - \bar{\theta}_b) \propto d\pi_u/d\tau$ and $\theta^{(i)} - \bar{\theta}^{(i)} \propto \bar{\theta}^{(i)} d\pi_u/d\tau$, the temperature $\theta^{(i)}$ can
 712 be replaced by $\bar{\theta}^{(i)}$ in front of the pressure term on the right-hand side of (5.10)

$$713 \quad z \geq 0 : \left[\frac{\partial \theta^{(i)}}{\partial \tau} - m(\tau) \frac{\partial \theta^{(i)}}{\partial z} - \frac{\partial^2 \theta^{(i)}}{\partial z^2} \right] \approx \frac{(\gamma - 1)}{\gamma} \left[q e^{-\bar{m}z} + (1 - q) \right] \epsilon \frac{d\pi_u}{d\tau}, \quad (7.2)$$

$$714 \quad \lim_{z \rightarrow \infty} \theta^{(i)}(z, \tau) = (1 - q) \left[1 + \epsilon \frac{\gamma - 1}{\gamma} \pi_u(\tau) \right], \quad \lim_{z \rightarrow \infty} \frac{\partial \theta^{(i)}}{\partial z} = 0, \quad (7.3)$$

715 where the ϵ^2 -terms have been neglected in the boundary conditions (5.11). Introducing the
 716 decomposition

$$717 \quad \theta^{(i)}(z, \tau) = \bar{\theta}^{(i)} + \delta \theta^{(i)}, \quad m(\tau) = \bar{m} + \delta m, \quad \bar{m} = e^{b\pi_u} \quad (7.4)$$

718 with, according to (6.6),

$$719 \quad z \geq 0 : \frac{\partial \bar{\theta}^{(i)}}{\partial \tau} = -q z e^{-\bar{m}z} \frac{d\bar{m}}{d\tau} + \epsilon(1 - q) \frac{(\gamma - 1)}{\gamma} \frac{d\pi_u}{d\tau}, \quad \frac{1}{\bar{m}} \frac{d\bar{m}}{d\tau} = b \frac{d\pi_u}{d\tau}, \quad (7.5)$$

720 equation (7.2) reads after subtracting $\partial\bar{\theta}^{(i)}/\partial\tau$ and $-\delta m\partial\bar{\theta}^{(i)}/\partial z = q\bar{m}e^{-\bar{m}z}\delta m$

$$721 \quad z \geq 0 : \left[\frac{\partial\delta\theta^{(i)}}{\partial\tau} - \bar{m} \frac{\partial\delta\theta^{(i)}}{\partial z} - \frac{\partial^2\delta\theta^{(i)}}{\partial z^2} \right] \approx -q\bar{m}e^{-\bar{m}z}\delta m \quad (7.6)$$

$$722 \quad +q \left[b\bar{m}ze^{-\bar{m}z} + \varepsilon \frac{(\gamma-1)}{\gamma} e^{-\bar{m}z} \right] \frac{d\pi_u}{d\tau},$$

723 with, according to the boundary conditions (7.3),

$$724 \quad \lim_{z \rightarrow \infty} \delta\theta^{(i)} = 0, \quad \lim_{z \rightarrow \infty} d\delta\theta^{(i)}/dz = O(\varepsilon^2). \quad (7.7)$$

725 Introducing the decomposition $Y = \bar{Y} + \delta Y$ into (4.13) using $\bar{Y} = e^{-\bar{m}z}$, $-\delta m\partial\bar{Y}/\partial z =$
726 $\bar{m}e^{-\bar{m}z}\delta m$ and $\partial\bar{Y}/\partial\tau = -\bar{m}ze^{-\bar{m}z}b\,d\pi_u/d\tau$ yields

$$727 \quad \left[\frac{\partial\delta Y}{\partial\tau} - \bar{m} \frac{\partial\delta Y}{\partial z} - \frac{\partial^2\delta Y}{\partial z^2} \right] \approx -\bar{m}e^{-\bar{m}z}\delta m + \bar{m}ze^{-\bar{m}z}b \frac{d\pi_u}{d\tau}, \quad \lim_{z \rightarrow \infty} \delta Y = 0. \quad (7.8)$$

728 The equation for $\delta Z \equiv \delta\theta^{(i)} - q\delta Y$ is free from the term $\delta m(\tau)$

$$729 \quad z \geq 0 : \left[\frac{\partial\delta Z}{\partial\tau} - \bar{m} \frac{\partial\delta Z}{\partial z} - \frac{\partial^2\delta Z}{\partial z^2} \right] \approx \varepsilon q \frac{(\gamma-1)}{\gamma} e^{-\bar{m}z} \frac{d\pi_u}{d\tau}, \quad \lim_{z \rightarrow \infty} \delta Z = 0. \quad (7.9)$$

730 Anticipating that δZ is of order $\varepsilon\,d\pi_u/d\tau$, neglecting terms of order $\varepsilon\,(d\pi_u/d\tau)^2$, the reduced
731 laminar flame speed $\bar{m} = e^{b\pi_u} + O(1/\beta)$ is treated as constant in (7.9). The unsteady term
732 $\partial\delta Z/\partial\tau < \delta Z$ can be neglected in front of $\partial\delta Z/\partial z$ and $\partial^2\delta Z/\partial z^2$ since $\partial/\partial z = O(1)$. After
733 integration $\int_z^\infty dz$, this yields

$$734 \quad z \geq 0 : \quad \bar{m}\delta Z + \frac{\partial\delta Z}{\partial z} = \varepsilon q \frac{(\gamma-1)}{\gamma} \frac{1}{\bar{m}} e^{-\bar{m}z} \frac{d\pi_u}{d\tau}$$

$$735 \quad \Rightarrow \quad \bar{m}\delta\theta_b + \frac{\partial\delta Z}{\partial z} \Big|_{z=0^+} = \varepsilon q \frac{(\gamma-1)}{\gamma} \frac{1}{\bar{m}} \frac{d\pi_u}{d\tau}, \quad (7.10)$$

736 where the boundary conditions $z = 0^+$: $\delta Y = 0$, $\delta Z = \delta\theta_b(\tau) \equiv \delta\theta^{(i)}(z=0, \tau)$ have been
737 used. Equation (7.10) can be checked by the small frequency limit of the Fourier transform
738 of (7.9). Using the relations $\partial\bar{\theta}^{(i)}/\partial z|_{z=0^-} = 0$ and $Y|_{z=0^-} = 0$ on the burned gas side, the
739 jump condition (3.11) takes the form

$$740 \quad \frac{\partial\theta^{(i)}}{\partial z} \Big|_{z=0^-} = \frac{\partial\theta^{(i)}}{\partial z} \Big|_{z=0^+} - q \frac{\partial Y}{\partial z} \Big|_{z=0^+} \Rightarrow \frac{\partial\delta\theta^{(i)}}{\partial z} \Big|_{z=0^-} = \frac{\partial\delta Z}{\partial z} \Big|_{z=0^+} \quad (7.11)$$

741 According to (7.10)-(7.11), the unsteadiness-induced modification of flame temperature $\delta\theta_b$,
742 $\theta_b = \bar{\theta}_b + \delta\theta_b$, is expressed in terms of the temperature gradient on the burned gas side of
743 the reaction sheet

$$744 \quad \bar{m}\delta\theta_b + \frac{\partial\delta\theta^{(i)}}{\partial z} \Big|_{z=0^-} = \varepsilon q \frac{(\gamma-1)}{\gamma} \frac{1}{\bar{m}} \frac{d\pi_u}{d\tau}. \quad (7.12)$$

745 The right-hand side of (7.12) is part of the perturbation of the flame temperature. The full
746 first order correction to $\beta(\theta_b - 1)$ requires to investigate the temperature in the burned-gas
747 flow ($z < 0$) for computing $\partial\delta\theta^{(i)}/\partial z|_{z=0^-}$.

748 7.1.2. Burned gas $z \leq 0$

749 For the analysis of the burned gas, one has to be back to (4.14). According to (6.1) and (6.5),
750 $\bar{\theta}^{(i)} - 1 = O(\varepsilon\pi_u)$ can be neglected in the factor of the pressure term on the right-hand side

751 of (4.14)

$$752 \quad z \leq 0 : \left[\frac{\partial \theta^{(i)}}{\partial \tau} - m(\tau) \frac{\partial \theta^{(i)}}{\partial z} - \frac{\partial^2 \theta^{(i)}}{\partial z^2} \right] = \varepsilon \frac{(\gamma - 1)}{\gamma} \left[\frac{\partial \pi_1}{\partial \tau} - m(\tau) \frac{\partial \pi_1}{\partial z} \right] [1 + O(\varepsilon)] \quad (7.13)$$

$$753 \quad \lim_{z \rightarrow -\infty} \theta^{(i)}(z, \tau) = 1, \quad \lim_{z \rightarrow -\infty} \pi_1(z, \tau) = 0, \quad (7.14)$$

754 where the boundary conditions (7.14) at infinity on the burned gas side is given by the
755 initial condition (hyperbolic problem). Neglecting $\varepsilon \partial^2 \pi_1 / \partial z^2$ in the burned gas, the energy
756 equation (7.13)-(7.14) can be written as an entropy equation

$$757 \quad z \leq 0 : \left[\frac{\partial}{\partial \tau} - \bar{m} \frac{\partial}{\partial z} - \frac{\partial^2}{\partial z^2} \right] s \approx 0, \quad s \equiv \left[\theta^{(i)} - \frac{(\gamma - 1)}{\gamma} \varepsilon \pi_1 \right], \quad \lim_{z \rightarrow -\infty} s = 1. \quad (7.15)$$

758 Anticipating that the unsteadiness-induced disturbances are of order $\varepsilon d\pi_u/d\tau$, the mass flux
759 m has been replaced by its unperturbed expression \bar{m} on the left-hand side of (7.15) since
760 the attention is limited to the leading order. Equation (7.15) shows how the entropy which is
761 generated across the flame structure during the flame acceleration

$$762 \quad s_b(\tau) \equiv s(z = 0, \tau) = \bar{\theta}_b(\tau) + \delta\theta_b(\tau) - (\gamma - 1)\varepsilon\pi_u(\tau)/\gamma \quad (7.16)$$

763 escapes the reaction zone from the hot side ($m > 0$). This leakage of entropy is the main
764 difference between a flame pushed from behind by a flow of burned gas and an adiabatic (and
765 impermeable) piston. The upstream boundary condition $\lim_{z \rightarrow -\infty} s = 1$ can also be viewed
766 as resulting from the damping of the transient variation of entropy by the heat conduction in
767 the (inert) burned gas. The solution to (7.15) is easily obtained using the Fourier transform
768 $s - 1 = e^{i\omega\tau} \tilde{s}_\omega(z)$ and the two relations (6.4) $\bar{\theta}_b - 1 = \varepsilon(1 - q)(\gamma - 1)\pi_u/\gamma$ and (7.16),
769 $s_b - 1 = \delta\theta_b - q(\gamma - 1)\pi_u/\gamma$

$$770 \quad z \leq 0 : \quad \tilde{s}_\omega(z) = \left[\delta\tilde{\theta}_b - q \frac{\gamma - 1}{\gamma} \varepsilon \tilde{\pi}_u \right] \exp \tilde{k} z, \quad (7.17)$$

$$771 \quad \tilde{k}(\omega) \equiv \frac{1}{2} \left[-\bar{m} + \sqrt{\bar{m}^2 + 4i\omega} \right] \approx \frac{i\omega}{\bar{m}} + \frac{\omega^2}{\bar{m}^3} + \dots \quad (7.18)$$

772 to give on the reaction sheet, using $\partial \tilde{s}_\omega / \partial z|_{z=0^-} \rightarrow \tilde{k}[\delta\tilde{\theta}_b - q(\gamma - 1/\gamma)\varepsilon\tilde{\pi}_u]$ and, in the low
773 frequency limit, $\tilde{k} \rightarrow (1/\bar{m})d/d\tau$,

$$774 \quad \frac{\partial s}{\partial z} \Big|_{z=0^-} = \frac{\partial \delta\theta^{(i)}}{\partial z} \Big|_{z=0^-} - q \frac{(\gamma - 1)}{\gamma} \varepsilon \frac{\partial \pi_1}{\partial z} \Big|_{z=0^-} \approx \frac{1}{\bar{m}} \frac{d\delta\theta_b}{d\tau} - q \frac{(\gamma - 1)}{\gamma} \frac{1}{\bar{m}} \varepsilon \frac{d\pi_u}{d\tau}. \quad (7.19)$$

775 This low frequency result corresponds to the undamped transport by the entropy wave
776 $\partial s / \partial \tau - \bar{m} \partial s / \partial z \approx 0$. The conduction-induced damping rate is of next order in the limit
777 of small frequency. This is similar to freely propagating acoustic waves in planar geometry.
778 In the limit $\varepsilon \ll 1$, the pressure gradient in the burned gas is negligible, the dominant
779 effect being through the increase rate in pressure (time derivative). To avoid any cumulative
780 effect that could induce acoustical instabilities reviewed in Clavin & Searby (2016), the ends
781 of the tube have been assumed sufficiently far away from the flame. Therefore, neglecting
782 $\varepsilon \partial \pi_1 / \partial z|_{z=0^-}$, equation (7.19) reads

$$783 \quad \text{burned gas:} \quad \frac{\partial \delta\theta^{(i)}}{\partial z} \Big|_{z=0^-} \approx \frac{1}{\bar{m}} \frac{d\delta\theta_b}{d\tau} - q \frac{(\gamma - 1)}{\gamma} \frac{1}{\bar{m}} \varepsilon \frac{d\pi_u}{d\tau}. \quad (7.20)$$

784 7.1.3. *Unsteady modification to the flame temperature.*

785 Introducing (7.20) into (7.12) leads

$$786 \quad \bar{m} \delta\theta_b + \frac{1}{\bar{m}} \frac{d\delta\theta_b}{d\tau} \approx 2q \frac{(\gamma-1)}{\gamma} \frac{1}{\bar{m}} \varepsilon \frac{d\pi_u}{d\tau}, \quad (7.21)$$

787 To first order, the time derivative on the left-hand side of (7.21) is negligible,

$$788 \quad \delta\theta_b \approx 2q \frac{(\gamma-1)}{\gamma} \frac{1}{\bar{m}^2} \varepsilon \frac{d\pi_u}{d\tau} = 2q \frac{(\gamma-1)}{\gamma} \exp[-2b\pi_u] \varepsilon \frac{d\pi_u}{d\tau}, \quad (7.22)$$

789 as it can be checked in the low frequency limit of the Fourier transform of (7.21),

$$790 \quad \delta\tilde{\theta}_b \approx 2q \frac{(\gamma-1)}{\gamma} \frac{1}{\bar{m}^2} \frac{i\omega}{1+i\omega/\bar{m}^2} \varepsilon \tilde{\pi}_u \approx 2q \frac{(\gamma-1)}{\gamma} \frac{1}{\bar{m}^2} \varepsilon i\omega \tilde{\pi}_u \left[1 - \frac{1}{\bar{m}^2} i\omega + O(\omega^2) \right]. \quad (7.23)$$

791 Thanks to the minus sign in front of $i\omega$ in the bracket, equation (7.23) describes a causal
792 response of the flame temperature to the time derivative of pressure. However, the causality
793 condition between the flame temperature $\theta_b(\tau) = \bar{\theta}_b(\tau) + \delta\theta_b(\tau)$ and the pressure $\pi_u(\tau)$ is
794 inverted,

$$795 \quad \theta_b(\tau) = 1 + \varepsilon(1-q) \frac{\gamma-1}{\gamma} \pi_u(\tau) + 2\varepsilon q \frac{(\gamma-1)}{\gamma} \exp[-2b\pi_u] \frac{d\pi_u}{d\tau} + O(\varepsilon^2), \quad (7.24)$$

$$796 \quad \beta(\theta_b - 1)/2 = b \left[\pi_u(\tau) + (\Delta\tau_\theta) d\pi_u(\tau)/d\tau + \dots \right] \approx b\pi_u(\tau + \Delta\tau_\theta), \quad (7.25)$$

$$797 \quad e^{\beta(\theta_b-1)/2} \approx e^{b\pi_u(\tau)} \left[1 + (\Delta\tau_\theta) b \frac{d\pi_u(\tau)}{d\tau} + \dots \right], \quad \Delta\tau_\theta = \frac{2q}{1-q} e^{-2b\pi_u} > 0. \quad (7.26)$$

798 where, according to (6.3), $b \equiv \beta\varepsilon(1-q)(\gamma-1)/2\gamma = O(1)$ and the τ -variation of π_u in the
799 coefficient $e^{-2b\pi_u}$ in front of $d\pi_u/d\tau$ on the right-hand side of (7.24) is negligible since it
800 introduces a correction of following order. Focusing the attention near the turning point, the
801 time delay is quasi-constant

$$802 \quad \Delta\tau_\theta \approx \frac{2q}{1-q} e^{-2b\pi_u^*} = O(1). \quad (7.27)$$

803 Equations (7.24)-(7.26) show that the flame temperature and the reaction rate at time τ are
804 related to the pressure at a later time $\tau + \Delta\tau_\theta$, $\Delta\tau_\theta > 0$. As we shall see later, such a non
805 causal response promotes an instability of the physical branch of the C-shaped curve "flame
806 velocity versus elongation".

807 7.1.4. *Unsteady modification to the mass flux.*

808 Anticipating that δY is of order $\varepsilon d\pi_u/d\tau \ll 1$, the unsteady term on the left-hand side of
809 (7.8) can be neglected to first order

$$810 \quad -\bar{m} \frac{\partial \delta Y}{\partial z} - \frac{\partial^2 \delta Y}{\partial z^2} \approx -\bar{m} e^{-\bar{m}z} \delta m + \bar{m} z e^{-\bar{m}z} b \frac{d\pi_u}{d\tau}. \quad (7.28)$$

811 Integration with the two boundary conditions $z = 0 : \delta Y = 0$ and $\lim_{z \rightarrow \infty} \delta Y = 0$ yields

$$812 \quad \delta Y = -e^{-\bar{m}z} z \delta m + \left[e^{-\bar{m}z} \frac{z^2}{2} + \frac{1}{\bar{m}} e^{-\bar{m}z} z \right] b \frac{d\pi_u}{d\tau}, \quad (7.29)$$

$$813 \quad \left. \frac{d\delta Y}{dz} \right|_{z=0^+} = -\delta m + \frac{1}{\bar{m}} b \frac{d\pi_u}{d\tau}. \quad (7.30)$$

814 According to the jump (3.10)-(3.11), the gradients on the flame sheet take the form

$$815 \quad \left. \frac{\partial \theta^{(i)}}{\partial z} \right|_{z=0^+} = -qe^{b\pi_u} \left[1 + \frac{\beta}{2} \delta \theta_b + \dots \right], \quad \left. \frac{\partial \delta \theta^{(i)}}{\partial z} \right|_{z=0^+} \approx -qe^{b\pi_u} \frac{\beta}{2} \delta \theta_b \quad (7.31)$$

$$816 \quad \left. \frac{\partial \delta \theta^{(i)}}{\partial z} \right|_{z=0^+} = q \left. \frac{\partial \delta Y}{\partial z} \right|_{z=0^+} + O(1/\beta). \quad (7.32)$$

817 After simplification by q , equations (7.31) and (7.32) read

$$818 \quad -e^{b\pi_u} \frac{\beta}{2} \delta \theta_b = \left. \frac{\partial \delta Y}{\partial z} \right|_{z=0^+} + O(1/\beta). \quad (7.33)$$

819 Introducing (7.25) into (7.33) and using (7.30) leads to the unsteady modification to the mass
820 flux across the reaction sheet defining the instantaneous laminar flame velocity relative to
821 the burned gas $U_b(\tau)$

$$822 \quad -e^{b\pi_u} \Delta \tau_\theta b \frac{d\pi_u}{d\tau} \approx -\delta m + \frac{1}{m} b \frac{d\pi_u}{d\tau} \quad \Rightarrow \quad \delta m \approx e^{-b\pi_u} \frac{1+q}{1-q} b \frac{d\pi_u}{d\tau}. \quad (7.34)$$

823 The modification of mass flux can be used to compute the variation of the speed of the
824 reaction sheet $U_P(t)$ when the back-flow $u_b(t)$ and the flame temperature are known.

825 *7.2. Dynamical effect of the unsteadiness of the inner structure*

826 The dynamics is governed by the ODE for $\pi_u(\tau)$ when the expressions of v_b and $\beta(\theta_b - 1)$
827 in terms of π_u are introduced into the master equation (5.18). The main difference with the
828 previous analysis of § 6 is that the unsteady flame temperature on the right-hand side of
829 (5.18) is no longer the temperature of the unburned gas simply shifted by the heat release as
830 in a steady laminar flame.

831 *7.2.1. Instantaneous back-flow model*

832 In a first step, assume for simplicity that the lateral flame (quasi-parallel to the lateral wall) are
833 quasi-steady, the unsteadiness being limited to the flame structure on the tip of the elongated
834 front. Neglecting heat loss at the wall, the temperature in the tongues of unburned gas
835 engulfed near the wall is assumed to be the same as in the flame on the tip of the elongated
836 front, this temperature being modified by the longitudinal compression wave propagating
837 ahead of the tip. This is an accurate approximation when the elongation is larger than the
838 acoustic wavelength. Then, the instantaneous back-flow (3.4) reads

$$839 \quad v_b(\tau)/S_i = (1 + \epsilon\tau)\bar{m}(\tau) = (1 + \epsilon\tau)e^{b\pi_u(\tau)} \approx e^{b\pi_u(\tau)} + \epsilon\tau e^{b\pi_u^*} + \dots \quad (7.35)$$

840 Introducing (7.26) and (7.35) into (5.18) yields

$$841 \quad S_i e^{b\pi_u(\tau)} + \epsilon\tau S_i e^{b\pi_u^*} - \left[S_i + q + \frac{\sqrt{1-q}}{\gamma} \pi_u(\tau) \right] \approx -qe^{b\pi_u(\tau)} - e^{-b\pi_u^*} \frac{2q}{1-q} b \frac{d\pi_u(\tau)}{d\tau}$$

842 which can be written

$$843 \quad [S_i(1 + \epsilon\tau) + q] e^{b\pi_u(\tau)} - \left[S_i + q + \frac{\sqrt{1-q}}{\gamma} \pi_u(\tau) \right] = -e^{-b\pi_u^*} \frac{2q}{1-q} b \frac{d\pi_u(\tau)}{d\tau}$$

844 and, using the notation (6.10)-(6.11),

$$845 \quad \zeta \exp \vartheta - \zeta_i - \vartheta/\tilde{b} = -\tilde{K}_\theta \frac{d\vartheta}{d\zeta}, \quad \text{where} \quad \tilde{K}_\theta \equiv \epsilon S_i e^{-b\pi_u^*} \frac{2q}{1-q} > 0 \quad (7.36)$$

$$846 \quad \frac{(\zeta - \zeta^*)}{\zeta^*} + \frac{(\vartheta^* - \vartheta)^2}{2} = -\tilde{\epsilon}_\theta \frac{d\vartheta}{d\zeta}, \quad \text{where} \quad \tilde{\epsilon}_\theta \equiv \tilde{b}\tilde{K}_\theta. \quad (7.37)$$

847 The difference with (6.22)-(6.23) is the sign on the right-hand side. The negative sign
848 obtained for the instantaneous back-flow shows that, according to the trajectories in the phase
849 space of (7.36)-(7.37), the unsteadiness of the inner flame structure promotes an instability
850 of the physical branch $\bar{\vartheta}_-(\zeta)$ of the quasi-steady solutions discussed in § 6.2.1. This would
851 be unfortunate for the study of the DDT when the elongation increases since the physical
852 branch of quasi-steady solutions could not be followed up to the vicinity of the turning point.
853 Hopefully, the delay in the back-flow restores the stability as shown now.

854 7.2.2. Delayed back-flow model

855 Still assuming that the lateral flames are in steady state, the non-dimensional expression of
856 the delayed back-flow is the same as (6.19). Introducing (7.26) and (6.19) into the master
857 equation (5.18) yields a non-dimensional ODE similar to (6.23)

$$858 \quad \frac{(\zeta - \zeta^*)}{\zeta^*} + \frac{(\vartheta^* - \vartheta)^2}{2} = \tilde{\epsilon} \frac{d\vartheta}{d\zeta}, \quad \text{where} \quad \tilde{\epsilon} \equiv \tilde{b}(\tilde{K}_w - \tilde{K}_\theta), \quad (7.38)$$

859 so that the phenomenology is the same as in § 6.3.2 provided $\tilde{K}_w > \tilde{K}_\theta$ which is typically
860 the case, see the text below (7.41).

861

862 7.2.3. Unsteady structure of the lateral flames

863 If the inner flame structure of the lateral flames is not in steady state, a delay is involved in the
864 radial flow of burned gas U_b feeding the longitudinal back-flow on the axis of the elongated
865 flame front. The unsteady laminar flame velocity U_b of the lateral flames is computed with
866 the first order disturbance of the mass rate across the reaction sheet $m(\tau)$ in (7.34). The
867 additional delay in the back-flow pushing the flame tip takes the form

$$868 \quad v_b/S_i \approx e^{b\pi_u(\tau)} + \epsilon\tau e^{b\pi_u^*} + e^{-b\pi_u^*} \frac{1+q}{1-q} b \frac{d\pi_u}{d\tau} + \dots \quad (7.39)$$

869 Introducing (7.26) and (7.39) into the master equation (5.18) yields an ordinary differential
870 equation for $\vartheta = b\pi_u$, namely for the pressure and/or the flame temperature similar to (7.38)
871 but involving an additional destabilizing term \tilde{K}_f

$$872 \quad \tilde{\epsilon} \equiv \tilde{b}(\tilde{K}_w - \tilde{K}_\theta - \tilde{K}_f), \quad \tilde{K}_f \equiv \epsilon S_i^2 e^{-b\pi_u} \frac{1+q}{1-q}. \quad (7.40)$$

873 The same equation as (6.23) is obtained in which K_w is replaced by $K_w - (K_\theta + K_f) > 0$.
874 The same finite-time singularity as that described at the end of § 6.3.2 is obtained, provided
875 the delays satisfy the following condition

$$876 \quad \tilde{K}_w > \tilde{K}_\theta + \tilde{K}_f \quad \Rightarrow \quad \frac{L/a_{\text{ref}}}{d_{\text{ref}}/U_{\text{ref}}} > e^{-2b\pi_u^*} \left[\frac{1}{S_i} \frac{2q}{1-q} + \frac{1+q}{1-q} \right] \quad (7.41)$$

877 which is verified for a length of the finger-like flame sufficiently elongated compared to
878 the flame thickness $L/d_{\text{ref}} > e^{-2b\pi_u^*}/\epsilon$. This is already the case for $\epsilon \approx 10^{-2}$ and a flame
879 elongation larger than a cell size of few centimetres (tube diameter).

880 **8. Discussion of the results and conclusion**

881 Starting with a small growth rate of elongation from a self-similar solution (quasi-steady
 882 solution for a constant elongation), the flame structure is suddenly blown off as a whole in
 883 finite time. This occurs for an elongation slightly larger than the critical elongation S^* of the
 884 quasi-steady solutions (burned gas flow and flame structure in steady state). In contrast to
 885 the solutions retaining only unsteadiness of the compression waves in the unburned gas, for
 886 which the singularity concerns the flow gradients only, a violent increase in pressure and flame
 887 temperature develops suddenly while the flame thickness shrinks to zero. The corresponding
 888 finite-time singularity is characterized by a dynamical saddle node bifurcation and develops
 889 independently of the precise expression of the delays involved in the unsteady flows provided
 890 the condition (7.41) is satisfied.

891 The finite time singularity is a consequence of a nonlinear thermal feedback-loop between
 892 the inner structure of the flame and the compressional heating by the downstream-running
 893 compression waves generated in the unburned gas by the accelerating flame acting as a semi-
 894 transparent piston. The acceleration is produced by the elongation-induced increase of the
 895 self-generated flow. The singularity appears systematically in the vicinity of the turning point
 896 whatever the elongation rate, as small as it may be. This is because the flame acceleration
 897 of the quasi-steady solution diverges at the turning point. The pre-conditioned state of
 898 unburned gas just ahead of the flame and just before the abrupt transition is characterized by
 899 a universal critical Mach number of the induced flow of unburned gas which is close to unity,
 900 in agreements with experiments and direct numerical simulations. This critical condition is
 901 all the easier to achieve in very energetic mixtures for an elongation which is not much larger
 902 than the tube radius. This could well be the case for the cellular structure of Rayleigh-Taylor
 903 unstable flame fronts of very energetic mixtures as those involved in supernovae SNIa.

904 The DDT mechanism is related to the finite-time singularity (6.26) of the solution to
 905 (6.25). This equation which is the normal form of a dynamical saddle node bifurcation has
 906 been obtained here by an expansion around the turning point. Therefore, the asymptotic
 907 behavior (6.27) is not guaranteed for the exact solution of equations (4.11)-(4.14) satisfying
 908 the boundary conditions (3.7)-(3.13). Nevertheless, the onset of a finite time singularity is not
 909 doubtful because unsteady terms of higher order than in (6.25) reinforce the singularity. This
 910 is illustrated by the divergence of the acceleration $d\vartheta/d\tau \propto 1/\sqrt{\tau^* - \tau}$ in (6.15) becoming
 911 $d\vartheta/d\tau \propto 1/(\tau_c - \tau)^2$ in (6.26) when unsteadinesses are taken into account. Moreover the
 912 singularity is even stronger when unsteady terms of following order are retained. For example,
 913 the divergence is sharper if the term dy'/dt' in (6.25) is replaced by a second order unsteady
 914 term d^2y'/dt'^2 (first Painlevé transcendent), $d\vartheta/d\tau \propto 1/(\tau_c - \tau)^3$. The numerical analyses of
 915 the one-dimensional problem (2.1)-(2.4) for the back flow models (3.4)-(3.7) to be published
 916 soon by Hernández-Sánchez and Denet confirm the finite time singularity.

917 The strong shock generated by the pressure runaway should lead quasi-instantaneously
 918 to the DDT. However, molecular dissipation and nonlinearities of the flow are essential
 919 in this ultimate phase of DDT. As for the formation of inert shock waves, microscopic
 920 length and time scales are involved (mean free path and inverse of the elastic collision
 921 frequency). Consequently this ultimate phase cannot be accurately described by macroscopic
 922 equations (2.1)-(2.4). In particular, the maximum shock intensity of the strong overdriven
 923 detonation appearing suddenly at the transition requires to solve the Boltzmann equation. The
 924 transverse extension of the explosion center should also play a role in that respect. However,
 925 once the overdriven detonation is formed, the subsequent relaxation toward the CJ regime
 926 (controlled by the rarefaction wave in the burned gas flow) can be described successfully
 927 by the macroscopic equations using the Rankine-Hugoniot jump conditions across the lead
 928 shock treated as a discontinuity since the induction length and the thickness of the exothermic

929 reaction zone behind the shock are macroscopic lengths. It is worth stressing once again
 930 that the singularity of the flame structure results from the generic divergence of the flame
 931 acceleration at the turning point, occurring for any growth rate of elongation (or of flame
 932 wrinkling) as small as it may be.

933 To summarize, the DDT mechanism presented in this article concerns a one-dimensional
 934 dynamics of reacting flow characterized by a rate of heat release highly sensitive to the
 935 temperature. Although the origin of the self-induced flow is multidimensional (increase in
 936 surface area of the elongated or wrinkled flame front), the DDT onset is a local process of
 937 a one-dimensional nature. This mechanism of transition concerns also turbulent wrinkled
 938 flames and/or unconfined cellular flames, the flame brush being considered as a chaotic array
 939 of elongated flames the tip of which is accelerated by the self-induced flow associated with
 940 the increase in surface area of the flame. In that sense, the DDT mechanism described here
 941 could have a certain degree of universality. This should be confirmed by direct numerical
 942 simulations keeping in mind the present analysis to analyze the results.

943

944 **Acknowledgements.** Yves Pomeau is acknowledged for enlightening discussions, especially concerning the
 945 dynamical saddle-node bifurcation. I am grateful to Grisha Sivashinsky for drawing my attention few years
 946 ago on the work of Joulin and Deshaies. I thank Misha Liberman for fruitful discussions on DDT and
 947 comments on the manuscript. I thank also Profs. Bruno Denet, Guido Lodato, Luc Vervisch and the Phd
 948 students Raúl Hernández-Sánchez and Hassan Tofaili for lively interactions during their numerical activities.

949 **Funding.** Partial financial support of *Agence National de la Recherche* (contract ANR-18-CE05-0030) is
 950 acknowledged

951 **Declaration of interests.** The author reports no conflict of interest.

952 **Appendix A. Linear dynamics of the flame for a pressure fluctuation**

953 The objective of this appendix is to study the stability of the two branches of steady state
 954 solutions obtained in § 6.1. To this end, it is worth considering first the response of a
 955 freely propagating planar flame to a uniform pressure fluctuation without limitation on the
 956 characteristic time of the pressure fluctuation. The attention is limited to the ZFK flame
 957 model in the limit of large activation energy $\beta \gg 1$.

958 *A.1. Response to a pressure fluctuation*

959 *A.1.1. Formulation*

960 Introducing the notation $f(\tau) \equiv \beta\varepsilon[(\gamma-1)/\gamma]\pi_u(\tau)$ for the reduced pressure $p/p_{\text{ref}} = 1 + \varepsilon\pi_u$
 961 and assuming $\beta\varepsilon$ of order unity in the limit $\beta \gg 1$, consider the solution to (4.13) and (4.16)

$$962 \quad \left[\frac{\partial Y}{\partial \tau} - m(\tau) \frac{\partial Y}{\partial z} - \frac{\partial^2 Y}{z^2} \right] = 0, \quad Y(z, \tau) \in [0, 1] \quad (\text{A } 1)$$

$$963 \quad \left[\frac{\partial \theta}{\partial \tau} - m(\tau) \frac{\partial \theta}{\partial z} - \frac{\partial^2 \theta}{z^2} \right] = \frac{\theta}{\beta} \frac{df}{d\tau} \quad (\text{A } 2)$$

964 satisfying the boundary conditions (3.9)-(3.11) on the reaction zone and

$$965 \quad z \rightarrow \infty : \quad Y = 0, \quad \frac{\partial \theta}{\partial z} = 0, \quad \theta = \theta_u(\tau) = (1 - q) + \frac{(1 - q)}{\beta} f(\tau) \quad (\text{A } 3)$$

966 in the unburned gas. The function $f(\tau) = \bar{f} + \delta f(\tau)$ is a given function of order unity while
 967 the flame velocity $m(\tau)$ and the flame temperature $\theta_b(\tau)$ are unknown functions of order

968 unity. According to the asymptotic method for large β , one introduces the decomposition,

$$969 \quad \theta = \theta_0 + \frac{\theta_1}{\beta}, \quad \theta_b = 1 + \frac{\theta_{b1}}{\beta}, \quad Y = Y_0 + \frac{Y_1}{\beta}, \quad m = m_0 + \frac{m_1}{\beta} \quad (\text{A } 4)$$

970 and, according to (3.10)-(3.11),

$$971 \quad \left. \frac{\partial \theta_0}{\partial z} \right|_{z=0^+} = -q \exp(\theta_{b1}/2), \quad \left. \frac{\partial \theta_{0,1}}{\partial z} \right|_{z=0^-} = \left. \frac{\partial \theta_{0,1}}{\partial z} \right|_{z=0^+} - q \left. \frac{\partial Y_{0,1}}{\partial z} \right|_{z=0^+}. \quad (\text{A } 5)$$

972 In the theory of flame, the instantaneous thermal flux on the hot side $\partial \theta / \partial z|_{z=0^-}$ to be
 973 introduced into the second jump condition (A 5) is given by the solution for the burned gas
 974 flow ($z < 0, Y = 1$) which is assumed adiabatic and uniform sufficiently far away from the
 975 flame. Equation (A 2) should then also be solved on the burned gas side for the boundary
 976 condition at infinity

$$977 \quad z \rightarrow -\infty : \quad \theta = 1 + \frac{1}{\beta} f(\tau). \quad (\text{A } 6)$$

978 In the linear response problem one consider a small fluctuation of the pressure $\delta f(\tau)$ and
 979 look for the linear solution $\delta \theta(z, \tau)$ and $\delta Y(z, \tau)$

$$980 \quad f = \bar{f} + \delta f, \quad \theta = \bar{\theta} + \delta \theta, \quad y = \bar{y} + \delta Y. \quad (\text{A } 7)$$

981 The unperturbed equations are

$$982 \quad \left[\frac{\partial \bar{Y}}{\partial \tau} - \bar{m} \frac{\partial \bar{Y}}{\partial z} - \frac{\partial^2 \bar{Y}}{\partial z^2} \right] = 0, \quad Y(z, \tau) \in [0, 1] \quad (\text{A } 8)$$

$$983 \quad \left[\frac{\partial \bar{\theta}}{\partial \tau} - \bar{m} \frac{\partial \bar{\theta}}{\partial z} - \frac{\partial^2 \bar{\theta}}{\partial z^2} \right] = 0 \quad (\text{A } 9)$$

$$984 \quad z \rightarrow \infty : \quad \bar{Y} = 1, \quad \bar{\theta} = \bar{\theta}_u, \quad \bar{\theta}_u \equiv (1 - q) + \frac{(1 - q)\bar{f}}{\beta}, \quad (\text{A } 10)$$

985 and the unperturbed solution is the ZFK solution $\bar{m} = e^{(1-q)\bar{f}/2}$

$$986 \quad z > 0 : \quad \bar{\theta} = qe^{-\bar{m}z} + \bar{\theta}_u, \quad Y = e^{-\bar{m}z}; \quad z < 0 : \quad \bar{\theta} = 1 + \frac{(1 - q)\bar{f}}{\beta}, \quad \bar{Y} = 1 \quad (\text{A } 11)$$

987 the unperturbed flame temperature being $z = 0 : \bar{\theta} = \bar{\theta}_b \equiv 1 + (1 - q)\bar{f}/\beta$.

988 A.1.2. Solution in the preheated zone

989 The linear equations in the preheated zone read

$$990 \quad z \geq 0 : \quad \left[\frac{\partial \delta Y}{\partial \tau} - \bar{m} \frac{\partial \delta Y}{\partial z} - \frac{\partial^2 \delta Y}{\partial z^2} \right] = -\delta m \bar{m} e^{-\bar{m}z}, \quad (\text{A } 12)$$

$$991 \quad \left[\frac{\partial \delta \theta}{\partial \tau} - \bar{m} \frac{\partial \delta \theta}{\partial z} - \frac{\partial^2 \delta \theta}{\partial z^2} \right] = -q \delta m \bar{m} e^{-\bar{m}z} + \frac{\bar{\theta}(z)}{\beta} \frac{d\delta f}{d\tau}, \quad (\text{A } 13)$$

$$992 \quad z \rightarrow \infty : \delta \theta = \frac{(1 - q)}{\beta} \delta f, \quad \delta Y = 0; \quad z = 0 : \delta \theta = \frac{\delta \theta_{b1}}{\beta}, \quad \delta Y = 0. \quad (\text{A } 14)$$

993 where the fluctuations of the flame temperature $\beta(\theta_b - \bar{\theta}_b) \equiv \theta_{b1}(\tau)$ and of the mass flux
 994 $\delta m(\tau)$ (flame velocity) are unknown. To leading order equations in the asymptotic analysis

995 for $\beta \gg 1$ the linear equations are

$$996 \quad z \geq 0 : \quad \left[\frac{\partial \delta Y_0}{\partial \tau} - \bar{m} \frac{\partial \delta Y_0}{\partial z} - \frac{\partial^2 \delta Y_0}{\partial z^2} \right] = -\delta m_0 \bar{m} e^{-\bar{m}z}, \quad (\text{A } 15)$$

$$997 \quad \left[\frac{\partial \delta \theta_0}{\partial \tau} - \bar{m} \frac{\partial \delta \theta_0}{\partial z} - \frac{\partial^2 \delta \theta_0}{\partial z^2} \right] = -q \delta m_0 \bar{m} e^{-\bar{m}z}, \quad (\text{A } 16)$$

$$998 \quad z \rightarrow \infty : \delta \theta_0 = 0, \quad \delta Y_0 = 0; \quad z = 0 : \delta \theta_0 = 0, \quad \delta Y_0 = 0. \quad (\text{A } 17)$$

999 Using the Fourier transform $\delta X = e^{i\omega\tau} \tilde{X}$ and the notation $\kappa_{\pm} \equiv \bar{m} \left[-1 \pm \sqrt{1 + 4i\omega/\bar{m}^2} \right] / 2$,
1000 $\text{Re}(\kappa_+) > 0$, $\text{Re}(\kappa_-) < 0$ the solution in the preheated zone takes the form

$$1001 \quad z \geq 0 : \quad \tilde{\theta}_0 = A_- e^{\kappa_- z} + A_+ e^{\kappa_+ z} + \frac{1}{\kappa_- - \kappa_+} \left[\frac{e^{-\bar{m}z} - e^{\kappa_+ z}}{\bar{m} + \kappa_+} - \frac{e^{-\bar{m}z} - e^{\kappa_- z}}{\bar{m} + \kappa_-} \right] q \bar{m} \tilde{m}_0, \quad (\text{A } 18)$$

1002 According to the boundary condition in the unburned gas, $A_+ = [(\kappa_- - \kappa_+)(\bar{m} + \kappa_+)]^{-1} q \bar{m} \tilde{m}_0$
1003 to eliminate the divergence at $z \rightarrow \infty$ and $A_- = \tilde{\theta}_0(0) - A_+$ with $\tilde{\theta}_0(0) = 0$, so that

$$1004 \quad q \tilde{Y}_0 = \tilde{\theta}_0 = \frac{e^{-\bar{m}z} - e^{\kappa_- z}}{(\bar{m} + \kappa_+)(\bar{m} + \kappa_-)} q \bar{m} \tilde{m}_0, \quad \left. \frac{d\tilde{\theta}_0}{dz} \right|_{z=0^+} = -\frac{1}{\bar{m} + \kappa_+} q \bar{m} \tilde{m}_0, \quad (\text{A } 19)$$

1005 with, according to the first jump condition in (A 5) $d\tilde{\theta}_0/dz|_{z=0^+} = -q\bar{m}\tilde{\theta}_{b1}/2$

$$1006 \quad \tilde{m}_0 = \frac{(\bar{m} + \kappa_+)}{2} \tilde{\theta}_{b1}. \quad (\text{A } 20)$$

1007 Therefore the solution requires the $1/\beta$ -modification to the flame temperature. The linear
1008 equations at the first order in the $1/\beta$ expansion are

$$1009 \quad \left[\frac{\partial \delta Y_1}{\partial \tau} - \bar{m} \frac{\partial \delta Y_1}{\partial z} - \frac{\partial^2 \delta Y_1}{\partial z^2} \right] = \delta m_1 \frac{\partial \delta Y_0}{\partial z}, \quad (\text{A } 21)$$

$$1010 \quad \left[\frac{\partial \delta \theta_1}{\partial \tau} - \bar{m} \frac{\partial \delta \theta_1}{\partial z} - \frac{\partial^2 \delta \theta_1}{\partial z^2} \right] = \delta m_1 \frac{\partial \delta \theta_0}{\partial z} + [q e^{-\bar{m}z} + (1 - q)] \frac{d\delta f}{d\tau}, \quad (\text{A } 22)$$

$$1011 \quad z \rightarrow \infty : \delta \theta_1 = (1 - q)\delta f, \quad \delta Y_1 = 0; \quad z = 0 : \delta \theta_1 = \theta_{b1}, \quad \delta Y_1 = 0. \quad (\text{A } 23)$$

1012 which can also be written in the form after having introduced $Z_1 \equiv \delta \theta_1 - (1 - q)\delta f - q\delta Y_1$

$$1013 \quad \left[\frac{\partial Z_1}{\partial \tau} - \bar{m} \frac{\partial Z_1}{\partial z} - \frac{\partial^2 Z_1}{\partial z^2} \right] = q e^{-\bar{m}z} \frac{d\delta f}{d\tau}, \quad (\text{A } 24)$$

$$1014 \quad z \rightarrow \infty : Z_1 = 0; \quad z = 0 : Z_1 = \theta_{b1} - (1 - q)\delta f, \quad (\text{A } 25)$$

1015 In Fourier transform $Z_1 = e^{i\omega\tau} \tilde{Z}_1(z)$, $\delta f(\tau) = e^{i\omega\tau} \tilde{f}$

$$1016 \quad \frac{d^2 \tilde{Z}_1}{dz^2} + \bar{m} \frac{d\tilde{Z}_1}{dz} - i\omega \tilde{Z}_1 = -q e^{-\bar{m}z} i\omega \tilde{f} \quad (\text{A } 26)$$

1017 the solution is

$$1018 \quad z \geq 0 : \quad \tilde{Z}_1 = B_- e^{\kappa_- z} + B_+ e^{\kappa_+ z} - \frac{1}{\kappa_- - \kappa_+} \left[\frac{e^{-\bar{m}z} - e^{\kappa_+ z}}{\bar{m} + \kappa_+} - \frac{e^{-\bar{m}z} - e^{\kappa_- z}}{\bar{m} + \kappa_-} \right] q i\omega \tilde{f}, \quad (\text{A } 27)$$

$$1019 \quad B_+ = \frac{-qi\omega \tilde{f}}{(\kappa_- - \kappa_+)(\bar{m} + \kappa_+)}, \quad B_- = \tilde{\theta}_{b1} - (1 - q)\tilde{f} - B_+ \quad (\text{A } 28)$$

1020 leading to

$$1021 \quad \tilde{Z}_1 = [\tilde{\theta}_{b1} - (1 - q)\tilde{f}]e^{\kappa_- z} - \frac{e^{-\bar{m}z} - e^{\kappa_- z}}{(\bar{m} + \kappa_+)(\bar{m} + \kappa_-)} q i \omega \tilde{f} \quad (\text{A } 29)$$

$$1022 \quad \left. \frac{d\tilde{Z}_1}{dz} \right|_{z=0^+} = \left. \frac{d(\tilde{\theta}_1 - q\tilde{Y}_1)}{dz} \right|_{z=0^+} = \kappa_- [\tilde{\theta}_{b1} - (1 - q)\tilde{f}] + \frac{q i \omega \tilde{f}}{\bar{m} + \kappa_+}. \quad (\text{A } 30)$$

1023 The solution is obtained by the second jump condition in (A 5),

$$1024 \quad \left. \frac{d\tilde{\theta}_1}{dz} \right|_{z=0^-} = \kappa_- [\tilde{\theta}_{b1} - (1 - q)\tilde{f}] + \frac{q i \omega \tilde{f}}{\bar{m} + \kappa_+} \quad (\text{A } 31)$$

1025 For the flame problem this requires to solve the burned gas flow ($z < 0$)

1026 A.1.3. Flame response

1027 In the burned gas equation(A 22) reduces to

$$1028 \quad z \leq 0 : \quad \left[\frac{\partial \delta \theta_1}{\partial \tau} - \bar{m} \frac{\partial \delta \theta_1}{\partial z} - \frac{\partial^2 \delta \theta_1}{\partial z^2} \right] = \frac{df}{d\tau} \Leftrightarrow \frac{d^2 \tilde{\theta}_1}{dz^2} + \bar{m} \frac{d\tilde{\theta}_1}{dz} - i \omega \tilde{\theta}_1 = -i \omega \tilde{f} \quad (\text{A } 32)$$

$$1029 \quad z \rightarrow -\infty : \tilde{\theta}_1 = \tilde{f}; \quad z = 0 : \tilde{\theta}_1 = \tilde{\theta}_{b1}. \quad (\text{A } 33)$$

1030 The solution is

$$1031 \quad z \leq 0 : \quad \tilde{\theta}_1 - \tilde{f} = (\tilde{\theta}_{b1} - \tilde{f}) e^{\kappa_+ z}, \quad \left. \frac{d\tilde{\theta}_1}{dz} \right|_{z=0^-} = \kappa_+ [\tilde{\theta}_{b1} - \tilde{f}] \quad (\text{A } 34)$$

1032 to give using (A 31)

$$1033 \quad (\kappa_+ - \kappa_-) [\tilde{\theta}_{b1} - \tilde{f}] = q \kappa_- \tilde{f} + q \frac{i \omega \tilde{f}}{\bar{m} + \kappa_+} \quad (\text{A } 35)$$

$$1034 \quad \tilde{\theta}_{b1} = \tilde{f} + \frac{q}{\kappa_+ - \kappa_-} \left[\kappa_- + \frac{i \omega}{\bar{m} + \kappa_+} \right] \tilde{f} \quad (\text{A } 36)$$

$$1035 \quad \tilde{\theta}_{b1} = \tilde{f} + \frac{q/\bar{m}}{\sqrt{1 + \frac{4i\omega}{\bar{m}^2}}} \left[-\frac{1 + \sqrt{1 + \frac{4i\omega}{\bar{m}^2}}}{2} \bar{m} + \frac{2/\bar{m}}{1 + \sqrt{1 + \frac{4i\omega}{\bar{m}^2}}} i \omega \right] \tilde{f} \quad (\text{A } 37)$$

$$1036 \quad \lim_{\omega \rightarrow 0} \tilde{\theta}_{b1} = \tilde{f} + q \left(1 - 2 \frac{i \omega}{\bar{m}^2} \right) \left[-\left(1 + \frac{i \omega}{\bar{m}^2} \right) + \frac{i \omega}{\bar{m}^2} \right] \tilde{f} + O(\omega^2 \tilde{f}) \quad (\text{A } 38)$$

$$1037 \quad = (1 - q) \tilde{f} + 2q \frac{i \omega}{\bar{m}^2} \tilde{f} + \dots \quad (\text{A } 39)$$

1038 corresponding to the quasi-steady solution (7.24) obtained by assuming a slow dynamics,

$$1039 \quad \delta \theta_{b1}(\tau) = (1 - q) \delta f(\tau) + \frac{2q}{\bar{m}^2} \frac{d \delta f(\tau)}{d\tau} + \dots \quad (\text{A } 40)$$

1040 According to (A 37), there is no effect when the heat release is zero (no gas expansion)
 1041 $\lim_{q \rightarrow 0} \tilde{\theta}_{b1} = \tilde{f}$ as it should be. The flame velocity is then obtained from (A 20) $\tilde{m}_0 =$
 1042 $(\bar{m} + \kappa_+) \tilde{\theta}_{b1} / 2$ to give in the small frequency limit $\lim_{\omega \rightarrow 0} \tilde{m}_0 = [(1 - q)/2][\tilde{f} + (i \omega / \bar{m}) \tilde{f}(1 +$
 1043 $q)/(1 - q)]$ in agreement with (7.34). Equations (A 20) and (A 37) are in agreement with
 1044 (4.7) in Clavin et al. (1990).

1045 A.1.4. *Response of the semi-transparent piston model*

1046 In this model the gas velocity u_b is imposed at the exit of the reaction zone with a zero
 1047 gradient of temperature (adiabatic semi transparent piston). Using the ZFK flame model this
 1048 is equivalent to impose a zero thermal flux on the burned gas side of the reaction sheet so that
 1049 the left-hand side of (A 31) is zero and the disturbance of the flame temperature is simply

$$1050 \quad \tilde{\theta}_{b1} = (1 - q)\tilde{f} - \frac{q i \omega \tilde{f}}{(\bar{m} + \kappa_+) \kappa_-} = (1 - q)\tilde{f} + \frac{q i \omega \tilde{f}}{\kappa_-^2} \quad (\text{A 41})$$

$$1051 \quad \lim_{\omega \rightarrow 0} \tilde{\theta}_{b1} = (1 - q)\tilde{f} + \frac{q}{\bar{m}^2} i \omega \tilde{f} + O(\omega^2) \quad (\text{A 42})$$

1052 It is worth noticing that, according to (A 40)-(A 42) the flame temperature and also the mass
 1053 flux (A 20) fluctuate in advance of the pressure fluctuation at low frequency.

1054 A.2. *Back flow induced acceleration*

1055 The flame temperature θ_b and the flows of burned and unburned gas on both sides of a ZFK
 1056 flame (v_b and v_u respectively) are related by the relation

$$1057 \quad v_b - v_u = -q e^{\beta(\theta_b - 1)/2}. \quad (\text{A 43})$$

1058 According to the developments in § 5.3, this relation is valid even for an unsteady inner
 1059 structure of the flame as soon as the flame Mach number is negligibly small $\varepsilon \ll 1$. When
 1060 the burned gas flow at the exit of the flame is accelerated from a steady state (labelled by the
 1061 subscript i) the upstream-running compression wave in the unburned gas makes the increase
 1062 in gas temperature and in flow just ahead of the flame related linearly to the pressure on the
 1063 flame $p/p_i - 1 = \varepsilon \pi_u(\tau)$

$$1064 \quad \theta_u(\tau) = (1 - q) + \frac{(\gamma - 1)}{\gamma} (1 - q) \varepsilon \pi_u(\tau), \quad v_u(\tau) = (S_i + q) + \frac{\sqrt{1 - q}}{\gamma} \pi_u(\tau) \quad (\text{A 44})$$

1065 where the initial conditions $\tau = 0 : \pi_u = 0, \theta_u = (1 - q)$ and $v_u = S_i + q$ have been used in
 1066 the first equation. The first relation in (A 44) is the adiabatic compression formula while the
 1067 second one comes from the upstream running compression wave.

1068 A.3. *Linear stability of the quasi-steady branches*

1069 Using the instantaneous back-flow model (3.4), the master equation (5.18) takes the form

$$1070 \quad S m - (S_i + q + \mu f) = -q e^{\beta(\theta_b - 1)/2}, \quad \mu \equiv \frac{\sqrt{1 - q}}{\varepsilon \beta(\gamma - 1)} = O(1). \quad (\text{A 45})$$

1071 A.3.1. *The two branches of quasi-steady solutions*

1072 When the inner structure of the flame is assumed in quasi-steady state, the flame temperature
 1073 is $\beta(\theta_b - 1) = (1 - q)f$ and the laminar flame speed reads $m = e^{\beta(\theta_b - 1)/2}$. Therefore the
 1074 quasi-steady solution \bar{f} corresponding to an elongation S is solution to

$$1075 \quad S \bar{m} - (S_i + q + \mu \bar{f}) = -q e^{\beta(\bar{\theta}_b - 1)/2}, \quad (\text{A 46})$$

$$1076 \quad \bar{m} = e^{\beta(\bar{\theta}_b - 1)/2}, \quad \beta(\bar{\theta}_b - 1) = (1 - q)\bar{f}, \quad \bar{m} = e^{(1 - q)\bar{f}/2}. \quad (\text{A 47})$$

1077 For a flame extension S given, the pressure \bar{f} is solution of a transcendental equation

$$1078 \quad (S + q) e^{(1 - q)\bar{f}/2} - (S_i + q + \mu \bar{f}) = 0. \quad (\text{A 48})$$

1079 This equation has two steady flame solutions $\bar{f}_-(S)$ and $\bar{f}_+(S)$ for $S < S^*$ and no solution
 1080 for $S > S^*$, S^* being a turning point $\bar{f}_-(S^*) = \bar{f}_+(S^*)$. The critical condition (labelled by the
 1081 superscript *) corresponds to the maximum of the curve $S(\bar{f})$, $dS/d\bar{f}|_{S=S^*} = 0$

$$1082 \quad (S^* + q)e^{(1-q)\bar{f}^*/2}(1-q)/2 - \mu = 0 \quad \Rightarrow \quad (S_i + q + \mu\bar{f}^*) = 2\mu/(1-q). \quad (\text{A } 49)$$

1083 Eliminating $S_i + q$ from (A 48) and (A 49) yields

$$1084 \quad (S + q)\bar{m}\frac{(1-q)}{2} - \mu = \mu\frac{(1-q)}{2}(\bar{f} - \bar{f}^*) \quad (\text{A } 50)$$

1085 An expansion of $S(\bar{f})$ around \bar{f}^* limited to the quadratic term yields

$$1086 \quad S - S^* \approx -\frac{(1-q)}{4}\frac{\mu}{\bar{m}^*}(\bar{f} - \bar{f}^*)^2, \quad f \equiv \beta\varepsilon[(\gamma - 1)/\gamma]\pi u. \quad (\text{A } 51)$$

1087 For a fixed elongation S , $S_i < S \leq S^*$, according to (A 45)-(A 47), the linear perturbation
 1088 associated with a pressure disturbance δf satisfies the linear equation

$$1089 \quad \text{linearisation for } S \text{ fixed : } S \delta m - \mu \delta f = -q\bar{m} \delta\theta_{b1}/2, \quad \mu \equiv \frac{\sqrt{1-q}}{\varepsilon\beta(\gamma - 1)} \quad (\text{A } 52)$$

1090 where the disturbance of the flame temperature $\delta\theta_{b1}$ is related to δf by the flame response
 1091 to pressure fluctuations.

1092 A.3.2. *Instability of the semi-transparent piston for $m = e^{(1-q)f/2}$ (model used by Raúl)*

1093 The attention is focused on the unsteadiness on the tip in this section. Assuming that the inner
 1094 structure of the lateral flames is quasi-steady, the radial mass flux leaving the flame skirt
 1095 is given by the Zeldovich analysis for a flame temperature simply shifted by the adiabatic
 1096 compression of the unburned gas. The burned gas flow velocity which is imposed on the
 1097 reaction sheet by the semi-transparent piston is $Se^{(1-q)f/2} = S\bar{m}[1 + (1-q)\delta f/2]$ in the linear
 1098 approximation $m = \bar{m} + \delta m$, $\delta m = (1-q)\bar{m}\delta f/2$. According to (A 52), a linear perturbation
 1099 around any solution corresponding to $S < S^*$ (there are two: \bar{f}_- and \bar{f}_+ , $\bar{f}_- < \bar{f}^* < \bar{f}_+$)
 1100 reads

$$1101 \quad \text{linearization for } S \text{ fixed : } S\bar{m}(1-q)\delta f/2 - \mu\delta f = -q\bar{m}\delta\theta_{b1}/2, \quad \bar{m} = e^{(1-q)\bar{f}/2}. \quad (\text{A } 53)$$

1102 into which the linear relation between the unsteady flame temperature on the tip $\delta\theta_{b1}$ and
 1103 δf should be introduced to determine the stability of the solution. For the semi-transparent
 1104 piston model, $\delta\theta_{b1}$ is given in terms of δf by (A 41). Looking for linear solutions in the form
 1105 $\delta f = e^{\sigma\tau}$, the dispersion relation controlling the stability of the flow for a fixed elongation
 1106 S is, according to (A 41) and (A 53),

$$1107 \quad S(1-q)\bar{m}/2 - \mu = -q(1-q)\bar{m}/2 - q\sigma\frac{2q/\bar{m}}{\left(1 + \sqrt{1 + 4\sigma/\bar{m}^2}\right)^2} \quad (\text{A } 54)$$

$$1108 \quad (S + q)(1-q)\bar{m}/2 - \mu = -2q^2\bar{m}\frac{\sigma/\bar{m}^2}{\left(1 + \sqrt{1 + 4\sigma/\bar{m}^2}\right)^2}, \quad \bar{m} = e^{(1-q)\bar{f}/2} \quad (\text{A } 55)$$

1109 According to (A 49), the left-hand side of (A 55) is zero at the critical elongation ($S = S^*$,
 1110 $\bar{f} = \bar{f}^*$) so that the linear growth rate is zero at the critical condition $\sigma|_{S=S^*} = 0$ as it should

1111 be for the usual exchange of stability at a turning point. Moreover, according to the derivative
1112 of (A 48) with respect to \bar{f} ,

$$1113 \quad \frac{dS}{d\bar{f}} e^{(1-q)\bar{f}/2} + (S+q)e^{(1-q)\bar{f}/2} \frac{(1-q)}{2} - \mu = 0 \quad (\text{A } 56)$$

1114 the physical branch of solutions $\bar{f}_-(S)$ which is characterized by $dS/d\bar{f} > 0$ corresponds to
1115 $(S+q)(1-q)\bar{m}/2 - \mu < 0$, in agreement with (A 50) for $\bar{f} < \bar{f}^*$. Therefore, according to
1116 (A 55), the physical branch of solutions $\bar{f}_-(S)$ is unstable $\sigma > 0$.

1117 A.3.3. *Instability of the instantaneous back-flow model of flame*

1118 According to (A 20), equation (A 52) reads

$$1119 \quad S(\bar{m} + \kappa^+) \delta\theta_{b1}/2 - \mu \delta f = -q\bar{m} \delta\theta_{b1}/2, \quad (\text{A } 57)$$

$$1120 \quad (S+q)\bar{m} \delta\theta_{b1}/2 - \mu \delta f = -S\kappa^+ \delta\theta_{b1}/2 \quad (\text{A } 58)$$

1121 where $\delta\theta_{b1}$ is given in (A 37) which can be written ($i\omega \rightarrow \sigma$) using the notation $s \equiv 4\sigma/\bar{m}^2$

$$1122 \quad \tilde{\theta}_{b1} = (1-q)\tilde{f} + \frac{q}{2} \left(\frac{-1 + \sqrt{1+s}}{\sqrt{1+s}} + \frac{s}{\sqrt{1+s}(1 + \sqrt{1+s})} \right) \tilde{f}$$

$$1123 \quad = (1-q)\tilde{f} + q \frac{s}{\sqrt{1+s}(1 + \sqrt{1+s})} \tilde{f} \quad (\text{A } 59)$$

1124 Then, equation (A 58) yields

$$1125 \quad (S+q)\bar{m} \frac{(1-q)}{2} - \mu = -(S+q)\bar{m} \frac{q}{2} \frac{s}{\sqrt{1+s}(1 + \sqrt{1+s})}$$

$$1126 \quad -S \frac{\bar{m}}{4} (\sqrt{1+s} - 1) \left[(1-q) + q \frac{s}{\sqrt{1+s}(1 + \sqrt{1+s})} \right] \quad (\text{A } 60)$$

$$1127 \quad \approx - \left[(S+q)\bar{m} \frac{q}{4} + S \frac{\bar{m}}{8} (1-q) \right] \frac{4}{\bar{m}^2} \sigma + O(\sigma^2) \quad (\text{A } 61)$$

1128 The left-hand side of (A 61) is zero at the critical elongation, see below (A 56). Then, for the
1129 same reason as before, the physical branch of solutions is unstable $\sigma > 0$.

REFERENCES

- 1130 BINDER, C.M. & ORSZAG, S.A. 1984 *Advanced mathematical methods for scientists and engineers* McGraw-
1131 Hill International Book Company.
- 1132 BYKOV, V., KOKSHAROV, A., KUZNETSOV, M. & ZHUKOV, V.P. 2022 Hydrogen-oxygen flame acceleration in
1133 narrow open ended channels *Combust. Flame.* **238** 111913.
- 1134 CLANET, C. & SEARBY, G. 1996 On the tulip flame phenomenon, *Combust. Flame.* **105** 225–238.
- 1135 CLAVIN, P. 2022 Finite-time singularity associated with the deflagration to detonation transition on the tip
1136 of an elongated flame-front in a tube *Combust. Flame.* **245** 112347.
- 1137 CLAVIN, P. & CHAMPION, M. 2022 Asymptotic solution of two fundamental problems in gaseous
1138 detonations *Combust. Sci. and Tech.* doi: 10.1080/00102202.2022.2041612.
- 1139 CLAVIN, P. & SEARBY, G. 2016 *Combustion waves and fronts in flows*. Cambridge University Press.
- 1140 CLAVIN, P. & TOFAILI, H. 2021 Formation of the preheated zone ahead of a propagating flame and the
1141 mechanisms underlying the deflagration-to-detonation transition, *Combust. Flame.* **232** 111522.
- 1142 DESHAIES, B. & JOULIN, G. 1989 Flame-speed sensitivity to temperature changes and the Deflagration-to-
1143 Detonation Transition, *Combust. Flame.* **77** 202–212.
- 1144 HERNÁNDEZ-SÁNCHEZ, R & DENET, B. 2023 *Private communication*

- 1145 HOUIM, W.H., OZGEN, A. & ORAN, E.S. 2016 The role of spontaneous waves in the deflagration-to-detonation
1146 transition in submillimetre channels, *Combust. Theory Model.* **20** 6 1068–1087.
- 1147 IVANOV, M.F., KIVERIN, A.D. & LIBERMAN, M.A. 2011 Hydrogen-oxygen flame acceleration and transition
1148 to detonation in a detailed chemical reaction model, *Phys. Rev E* **83** 056313.
- 1149 KAGAN, L. & SIVASHINSKY, G. 2017 Parametric transition from deflagration to detonation: Runaway of fast
1150 flames, *Proc. Combust. Inst.* **36** 2709–2715.
- 1151 KUZNETSOV, M., LIBERMAN M.A. & MATSUKOV, I. 2010 Experimental study of the preheated zone formation
1152 and deflagration to detonation transition, *Combust. Sci. and Tech.*, **182** 1628–1644.
- 1153 LEE, J. 2008 *The detonation phenomena*. Cambridge University Press.
- 1154 LIBERMAN, M.A., IVANOV, M.F., KIVERIN, A.D., KUZNETSOV, M.S., CHUKALOVSKY, A.A. & RAKIMOVA,
1155 T.V. 2010 Deflagration-to-detonation transition in highly reactive mixtures, *Acta Astronautica* **67**
1156 688-701.
- 1157 PETERS, D.R., LE BERRE M. & POMEAU, Y. 2012 Prediction of catastrophes: A experimental model, *Pys.*
1158 *Rev. E.*, **86** 026207.
- 1159 SHCHELKIN, K.I. & TROSHIN, YA.K. 1965 *Gasdynamics of combustion*. Mono Book Corp.
- 1160 STROGATZ, S.H. 1994 *Nonlinear dynamics and chaos*. Perseus Books Publishing, LLC.
- 1161 URTIEW, P.A & OPPENHEIM, A.K 1966 Experimental observations of the transition to detonations in an
1162 explosive gas, *Proc. R. Soc. London A* **295** 13–28.
- 1163 WU, M., BURKE, M.P., SON S.F. & YETTER, R.A. 2007 Flame acceleration and the transition to detonation
1164 of stoichiometric ethylene/oxygen in microscale tubes, *Proc. Comb. Inst.* **31** 2429–2436.
- 1165 WU, M. & WANG, C. 2011 Reaction propagation modes in millimeter-scale tubes for ethylene/oxygen
1166 mixtures, *Proc. Comb. Inst.* **33** 2287–2293.
- 1167 ZELDOVICH, YA.B. 1980 Regime classification of an exothermic reaction with nonuniform initial conditions
1168 *Combust. Flame* **39** 211–214.